

NACA RM No. E8107

Unavailable

Inactive

~~CLASSIFICATION CHANGED~~

To ~~CONFIDENTIAL~~ **NACA**

By authority of *Pres. Release*
Pres. Order No. 2292

Date *January 2, 1954* *JRE-1-15-54*

RESEARCH MEMORANDUM

Inactive

EXPERIMENTAL PRESSURE DISTRIBUTION ON FUSELAGE

NOSE AND PILOT CANOPY OF SUPERSONIC AIRPLANE

AT MACH NUMBER 1.90

By DeMarquis D. Wyatt

Flight Propulsion Research Laboratory
Cleveland, Ohio

7/1/54
CLASSIFICATION CHANGED

UNCLASSIFIED

NACA Release

YRN-126

By authority of

1/15/54

Date *effective Apr. 15, 1954*

**NATIONAL ADVISORY COMMITTEE
FOR AERONAUTICS LIBRARY COPY
WASHINGTON**

OCT 15 1948

JAN 15 1954

LANGLEY AERONAUTICAL LABORATORY
LIBRARY, NACA
LANGLEY FIELD, VIRGINIA

Unavailable

SPECIAL RELEASE
TRANSMITTED ON
NOT TO BE INDEXED, REPRODUCED, OR GIVEN FURTHER
CITATION

This document contains classified information affecting the National Defense of the United States within the meaning of the Espionage Act, USC 8031 and 22. Its transmission or the revelation of its contents in any manner to an unauthorized person is prohibited by law. Information so classified may be imparted only to persons in the military and naval services of the United States, appropriate civilian officers and employees of the Federal Government who have a legitimate interest therein, and to United States citizens of known loyalty and discretion who of necessity must be permitted to have access to it.

NACA RM No. E8107

EXPERIMENTAL PRESSURE DISTRIBUTION ON FUSELAGE
NOSE AND PILOT CANOPY OF SUPERSONIC AIRPLANE
AT MACE NUMBER 1.90

DeMarquis D. Wyatt,
Aeronautical Research Scientist.

Approved:

John C. Evvard,
Physicist.

Abe Silverstein,
Aeronautical Research Scientist.
jgm



NATIONAL ADVISORY COMMITTEE FOR AERONAUTICS

RESEARCH MEMORANDUMEXPERIMENTAL PRESSURE DISTRIBUTION ON FUSELAGENOSE AND PILOT CANOPY OF SUPERSONIC AIRPLANE

AT MACH NUMBER 1.90

By DeMarquis D. Wyatt

SUMMARY

An investigation of the pressure distribution on the fuselage nose and the pilot canopy of 8 supersonic airplane model has been conducted at 8 Mach number of 1.90 over 8 wide range of angles of attack and yaw. The pressure distributions conformed to anticipated trends. Boundary-layer separation apparently occurred from the upper surface at angles of attack above 24° and from the lower surface at -15° . No separation from the sides of the fuselage was evident at yaw angles up to 12° .

INTRODUCTION

Theoretical methods are available for the calculation of pressure distributions on conical bodies and axially symmetric non-conical bodies in 8 supersonic stream, but no satisfactory methods are available for the treatment of arbitrary nonconical bodies without axial symmetry. In order to determine the pressure distribution on 8 nonconical airplane fuselage without axial symmetry, a model was experimentally investigated. Data were obtained over 8 wide range of angles of attack and yaw at 8 Mach number of 1.90 in the NACA Cleveland 18- by 18-inch supersonic tunnel.

APPARATUS AND PROCEDURE

The test-section Mach number in the 18- by 18-inch supersonic tunnel in the region in which the model was located was 1.90 ± 0.02 , as determined by a calibration of the tunnel. Tunnel-inlet conditions were maintained at a stagnation temperature of $150^\circ \pm 10^\circ \text{ F}$ and a dew-point temperature of $-10^\circ \pm 10^\circ \text{ F}$. The Reynolds number of the model, based on the model length, was approximately 3.8×10^6 .

1025
Photographs of the brass model of the fuselage nose and the pilot canopy of a supersonic airplane are presented in figure 1. A sketch of the model showing principal dimensions and typical cross sections is presented in figure 2. The length of the model over which pressures were measured was 13.50 inches. Static-pressure orifices of 0.013-inch diameter were located along several longitudinal body lines of the model. The orifice locations are given in table I in terms of the ratio x/L and the angle θ , where x is the distance from the tip of the model to the orifice, L is the length of the model over which pressures were measured (13.50 inches), and θ is the angle between the top of the model and the orifice, measured in a clockwise direction looking forward. Pressures were recorded from a multiple-tube manometer board using tetrabromoethane as a fluid and were read to the nearest 0.05 inch of fluid.

The model was supported from the rear by a cylindrical body that was pinned to a strut passing through the bottom of the tunnel (fig. 1(a)). The strut was split and could be adjusted from outside the tunnel to vary the angle of attack of the model during operation of the tunnel. The angle of attack of the model was determined from cathetometer measurements taken during operation. For variations in yaw angle, the model was rotated 90° in the mounting from the position shown in figure 1(8).

The investigation was conducted at 0° angle of yaw over an angle of attack range from -15° to 30° , and at 0° , 5° , and 10° angles of attack over an angle of yaw range from -15° to 15° . Adaptor mountings were inserted between the model and the support body to give the 5° and 10° angles of attack for the investigation of yaw effects at angles of attack. The model was centered in the tunnel at 0° deflection for all phases of the investigation in which the yaw angle was varied and for runs at negative angles of attack and 0° yaw. In order to avoid tunnel-wall interferences, the model was lowered about 3 inches in the tunnel for positive angle of attack at 0° yaw angle.

RESULTS AND DISCUSSION

Data are presented in tables II to V in the form of pressure coefficient C_p at each orifice for each condition investigated. The pressure coefficient is defined by the equation

$$C_p = \frac{p - p_0}{q_0} \quad (1)$$

where p is the local surface pressure, p_0 is the free-stream static pressure, and q_0 is the free-stream dynamic pressure.

The data presented in table II were obtained with the model at two vertical positions in the tunnel. Pressure coefficients measured at 0° angle of attack varied as much as 0.08 for corresponding orifices between the two runs. Check run substantiated this discrepancy. The variable yaw angle tests were made with the model centered in the tunnel in the same vertical position as for the negative angle of attack tests, but the data for 0° angle of yaw (tables III to V) show good agreement with the data obtained at positive angle of attack. Because of the agreement between the data for positive angles of attack and data for variable yaw angles, the data in table II for negative angle of attack are believed to be incorrect.

Typical schlieren photographs of the model are presented in figure 3 for conditions of 0° yaw angle and several angles of attack. An apparent pronounced boundary-layer separation from the top (expansion) surface of the model was observed at angles of attack of 30° and 24° (figs. 3(a) and 3(b)). Inconsistent variations in the pressure coefficients measured on the upper surface that were observed for these conditions are attributed to the apparent separation.

The boundary layer did not appear to separate from the body at the lower angles of attack, although the layer was appreciably thickened about halfway between the tip and the pilot canopy at 18° angle of attack (fig. 3(c)). Below an angle of attack of 18° , no thickening of the boundary layer was evident (figs. 3(d) to 3(f)). The boundary-layer growth on the lower surface was moderate at -6° angle of attack (fig. 3(g)), but separation appeared to occur near the tip at -15° (fig. 3(h)).

The apparent line of discontinuity in the separated region adjacent to the upper surface of the body at 24° angle of attack (fig. 3(b)) cannot be explained. This line was noticeable near the canopy at 21° angle of attack and persisted up to 27° angle of attack. The line was not transient, being visible on the schlieren screen during steady observation of the flow.

The schlieren photographs in figure 4 are typical of those obtained for all runs at variable yaw angle. operation up to yaw angles of 12° caused no appreciable thickening or observable separation of the boundary layer.

Pressure distributions along longitudinal planes on the model are plotted in figure 5 from the data in table II for a representative range of angles of attack at 0° yaw angle. Data for 0° angle of attack were taken from only the positive angle of attack run. The pressure coefficient trends conformed to the anticipated trends. Because of flow expansion along the nonconical body, the pressures decreased in a rearward direction. Pressures increased appreciably on the canopy as compared with the fuselage nose because of the shock originating from the canopy. The canopy had no influence on the pressures on the lower part of the body.

Longitudinal pressure distributions are plotted in figures 6 to 8 for a range of yaw angles at 0° , 5° , and 10° angles of attack, respectively. Because of body symmetry about the vertical plane through the centerline of the body, it was expected that the values of pressure coefficient measured at the intersection of this plane with the top and the bottom of the body would be the same for both positive and negative yaw angles. The experimentally measured pressure coefficients were the same for positive and negative angles of yaw, indicating uniform conditions in the tunnel air stream.

Radial pressure distributions at two locations on the body are presented in figures 9 to 12. Data for these figures were obtained from the faired curves of figures 5 to 8. The pressure distribution at $x/L = 0.148$ (section A-A, fig. 2) was qualitatively typical of the pressure distribution at any point on the fuselage nose ahead of the canopy. The distribution at $x/L = 0.898$ (section E-E, fig. 2) was similarly typical of the flow over the rear section of the canopy. Because of the body symmetry about the vertical centerline, curves are presented for only the negative angles of yaw in figures 10 to 12; the curves of the data for positive angles of yaw are mirror images of the curves shown.

Pressure distributions on the flat pilot canopy are indicated in figures 13 to 16 for representative test conditions. The rearward orifices were located on the right side of the canopy, but the appropriate data are transposed in these figures to indicate the pressures on the left canopy surface. A double set of values is given at one orifice location. The upper value was measured on the left and the lower value was measured on the right canopy surface.

SUMMARY OF RESULTS

The following results were obtained from an investigation of the pressure distribution on the fuselage nose and the pilot canopy of a supersonic airplane model at a Mach number of 1.90 and a Reynolds number of 3.8×10^6 :

1. Measured *longitudinal* pressure distribution trends conformed to anticipated trends. Pressures decreased in a rearward direction on the fuselage nose, corresponding to a flow expansion about the nonconical body. The compression shock originating from the canopy increased pressures on the canopy as compared with the fuselage nose. The canopy had no influence on pressures on the lower surface of the fuselage.

2. Apparent boundary-layer separation from the top surface of the body was observed at angles of attack above 24° and from the bottom surface at -15° angle of attack.

Flight Propulsion Research Laboratory,
National Advisory Committee for Aeronautics,
Cleveland, Ohio, September 7, 1948.

TABLE I - ORIFICE LOCATIONS ON MODEL

Radial location θ , (deg)	Longitudinal location, x/L								
0	0.074	0.185	0.296	0.406	0.516	0.630	0.743	0.852	0.963
30	a.889	a.926	a.963	-----	-----	-----	-----	-----	-----
45	.111	.222	.333	.444	.556	.667	.778	a.889	a.926
60	a.889	a.926	a.963	-----	-----	-----	-----	-----	-----
180	.093	.204	.315	.426	.537	.648	.759	.870	.982
225	.130	.241	.352	.463	.574	.685	.796	.908	-----
270	.148	.259	.370	.481	.592	.704	.815	.926	-----
300	a.852	-----	-----	-----	-----	a-----	--mm--	--mm--	-----
315	a.852	--we-	-----	-w-s-	-----	----w	---w--	-----	-----
330	a.852	--w--	-----	---m-	---a-	--a--	-----	-----	-----
340	a.815	a.852	-----	e--m-	-w---	B-L--	-a----	-----	-----
350	a.778	a.815	a.852	-m---	-----	w--m-	--I---	-----	-----
355	a.778	a.815	--I--	-----	-----	--m--	-----	-----	-----

^aOrifice on canopy.

NACA

TABLE II - TABULATED PRESSURE COEFFICIENTS AT 0° YAW ANGLE FOR RANGE OF ANGLES OF ATTACK

Angle of Attack, α	30	27	24	21	18	15	12	9	6	3	0	0	-3	-6	-9	-12	-15
θ (deg)	Pressure coefficient, C_p																
x/L																	
0	.074	-.114	-.126	-.099	-.048	-.033	-.011	-.008	-.005	.012	.009	.028	.054	.062	.126	.144	.174
.184	-.196	-.113	-.077	-.053	-.014	-.012	-.008	-.008	-.003	.015	.010	.026	.046	.071	.121	.170	.200
.296	-.283	-.164	-.077	-.041	-.023	-.025	-.018	-.013	-.021	-.001	.016	.009	.024	.050	.080	.124	.189
.408	-.282	-.177	-.086	-.067	-.028	-.025	-.017	-.015	-.012	-.010	.008	.006	.025	.044	.073	.116	.172
.518	-.293	-.271	-.111	-.077	-.041	-.024	-.025	-.018	-.015	-.011	.004	.011	.018	.044	.078	.109	.162
.630	-.302	-.304	-.144	-.087	-.049	-.034	-.033	-.031	-.015	-.021	-.014	.008	.015	.040	.070	.098	.156
.741	-.288	-.345	-.125	-.009	.012	.014	.018	.017	.020	.025	.049	.064	.080	.107	.142	.181	.236
.852	-.278	-.303	-.151	.013	.021	.009	.005	.007	.014	.018	.038	.078	.102	.134	.168	.213	.263
.963	-.190	-.290	-.137	-.068	-.014	.008	.003	.014	.030	.026	.031	.052	.071	.099	.134	.173	.219
30	.889	-.227	-.293	-.229	-.191	-.199	-.029	.070	.073	.083	.087	.094	.138	.127	.125	.132	.148
.926	-.239	-.298	-.238	-.205	-.189	-.029	.050	.059	.073	.081	.091	.116	.127	.143	.150	.165	.191
.963	-.237	-.283	-.243	-.213	-.177	-.050	.029	.037	.064	.066	.082	.109	.123	.133	.148	.164	.191
45	.111	-.241	-.236	-.208	-.176	-.142	-.093	-.025	.006	.016	.040	.053	.077	.093	.090	.106	.106
.222	-.275	-.264	-.236	-.228	-.193	-.110	-.085	-.030	-.003	.012	.008	.021	.033	.042	.060	.088	.105
.333	-.290	-.274	-.237	-.226	-.194	-.139	-.067	-.021	-.018	.004	.016	.007	.014	.028	.041	.061	.097
.444	-.297	-.280	-.237	-.231	-.178	-.116	-.049	-.040	-.023	-.014	.003	.006	.012	.022	.030	.048	.080
.555	-.303	-.304	-.235	-.223	-.199	-.116	-.060	-.030	-.024	-.014	0	.010	.013	.031	.041	.067	.082
.666	-.292	-.308	-.256	-.217	-.190	-.108	-.054	-.040	-.030	-.025	-.018	.006	.009	.019	.023	.040	.068
.778	-.300	-.315	-.248	-.219	-.194	-.132	-.028	-.028	-.017	-.004	-.001	.015	.021	.028	.039	.054	.074
.889	-.272	-.291	-.209	-.144	-.127	-.117	.099	.099	.106	.110	.128	.144	.137	.136	.138	.141	.159
.926	-.274	-.298	-.213	-.123	-.095	-.086	.084	.086	.096	.101	.119	.147	.146	.148	.149	.157	.176
.963	-.265	-.289	-.258	-.142	-.093	-.135	.060	.065	.080	.088	.098	.123	.124	.134	.144	.152	.174
60	.889	-.246	-.289	-.230	-.139	-.114	-.116	.042	.050	.066	.078	.089	.116	.124	.133	.147	.162
.926	-.236	-.293	-.226	-.136	-.077	-.060	0	.065	.082	.089	.100	.123	.126	.124	.124	.127	.141
.963	-.234	-.291	-.198	-.160	-.083	.002	.002	.066	.070	.081	.088	.113	.118	.120	.127	.137	.153
180	.093	.677	.693	.618	.444	.399	.328	.261	.190	.133	.093	.054	.085	.055	.031	-.001	-.023
.204	.595	.543	.486	.404	.319	.249	.194	.143	.094	.049	.021	.031	.011	.004	.012	-.039	-.040
.315	.619	.586	.440	.359	.286	.224	.163	.110	.074	.041	.009	.019	.001	-.011	.019	-.026	-.051
.426	.561	.476	.399	.322	.251	.186	.134	.086	.049	.023	-.004	.004	.013	.023	.026	-.040	-.058
.537	.507	.454	.377	.302	.229	.168	.118	.075	.040	.015	-.004	.004	.012	.012	.026	-.040	-.059
.648	.517	.436	.361	.289	.218	.160	.109	.068	.036	.013	-.003	.002	.012	.016	.022	-.040	-.058
.759	.496	.417	.340	.267	.200	.140	.094	.055	.022	.001	-.011	0	.012	.019	.029	-.049	-.061
.870	.503	.417	.342	.267	.204	.144	.097	.061	.032	.006	-.005	.015	.002	.019	.036	-.036	-.052
.982	.490	.417	.348	.277	.202	.139	.092	.052	.026	.009	-.003	.010	.006	.004	.003	-.017	-.040
225	.130	.282	.241	.201	.184	.151	.117	.093	.082	.072	.051	.036	.051	.028	.007	-.032	-.070
.241	.246	.207	.171	.130	.088	.059	.045	.042	.039	.026	.015	.025	.009	-.015	.045	.082	-.110
.352	.229	.177	.138	.101	.072	.043	.025	.016	.019	.021	.007	.017	.001	-.021	.064	.077	-.115
.463	.186	.144	.105	.067	.036	.012	-.008	-.002	.002	.006	0	.005	.009	.032	.052	.072	-.107
.574	.179	.136	.095	.056	.024	.002	-.012	-.012	-.004	.003	.002	.007	.010	.029	.047	.061	-.094
.685	.146	.103	.067	.030	0	.024	.024	.024	-.014	-.008	-.002	.005	.008	.025	.046	.068	-.093
.796	.125	.084	.048	.015	-.016	-.038	.045	.043	-.021	-.014	-.008	.010	.007	.030	.048	.068	-.098
.908	.162	.129	.099	.071	.021	-.011	.014	.013	.010	.019	.024	.022	.002	-.021	.039	.053	-.087
270	.148	-.219	-.215	-.193	-.171	-.153	-.115	-.080	-.045	-.003	.001	.027	.029	.030	.035	.032	.006
.259	-.194	-.198	-.191	-.187	-.177	-.156	-.106	-.064	-.035	-.004	.005	.006	.012	.008	.006	.015	-.021
.370	-.179	-.179	-.173	-.168	-.174	-.153	-.117	-.068	-.028	-.005	.013	.019	.016	.010	.002	.016	-.023
.481	-.174	-.167	-.167	-.154	-.165	-.146	-.113	-.075	-.038	-.016	-.002	.004	.002	.001	.016	.027	-.031
.592	-.177	-.155	-.160	-.157	-.157	-.160	-.120	-.081	-.045	-.021	-.008	.004	.003	.008	.029	.036	-.060
.704	-.202	-.155	-.163	-.173	-.161	-.169	.123	.093	.041	.025	-.016	.004	.002	.004	.019	.042	-.062
.815	-.202	.147	-.175	-.179	-.155	-.136	.132	.075	.046	.037	-.017	.005	.007	.010	.022	.039	-.062
.926	-.132	-.043	-.042	-.052	-.032	-.001	.027	.067	.091	.101	.103	.117	.124	.089	.056	.020	-.008
300	.852	-.125	-.025	-.041	-.052	-.087	.099	.017	.102	.126	.133	.128	.154	.153	.150	.148	.149
.915	-.135	-.042	-.075	-.068	-.102	-.108	.003	.102	.118	.122	.118	.154	.141	.147	.157	.151	.175
.952	-.178	-.066	-.121	-.094	-.123	-.063	.088	.085	.093	.098	.092	.126	.127	.141	.155	.161	.183
340	.815	-.141	-.100	-.156	-.140	-.178	.021	.073	.061	.064	.069	.067	.137	.146	.151	.154	.171
.852	-.164	-.099	-.161	-.150	-.168	.042	.075	.067	.072	.070	.072	.106	.115	.137	.154	.168	.195
350	.778	-.097	-.151	-.128	-.146	-.060	.047	.046	.041	.042	.042	.060	.085	.086	.101	.118	.143
.815	-.056	-.197	-.129	-.143	-.034	.063	.057	.052	.050	.054	.061	.131	.121	.131	.145	.174	.226
.852	-.082	-.198	-.141	-.148	-.021	.056	.045	.043	.045	.045	.057	.094	.114	.139	.163	.187	.222
355	.778	-.063	-.225	-.102	-.091	.006	.047	.043	.038	.036	.036	.054	.077	.089	.109	.131	.163
.815	-.014	-.241	-.108	-.070	.032	.050	.047	.041	.039	.045	.048	.118	.112	.130	.153	.189	.245

TABLE III - TABULATED PRESSURE COEFFICIENTS AT 0° ANGLE OF ATTACK
FOR RANGE OF YAW ANGLES

Angle of yaw, γ deg		Pressure coefficient, C_p											
θ (deg)	x/L	12	9	6	3	0	-3	-6	-9	-12			
0	.074	-.134	-.072	-.007	.044	.051	.030	-.018	-.080	-.134			
	.185	-.152	-.101	-.036	.015	.025	.003	-.043	-.101	-.152			
	.286	-.150	-.119	-.059	-.009	.004	-.018	-.062	-.106	-.147			
	.408	-----	-----	-.061	-.015	0	-.020	-.063	-.102	-.139			
	.518	-.133	-.100	-.062	-.019	.004	-.017	-.052	-.088	-.128			
	.630	-.121	-.089	-.071	-.028	-.011	-.040	-.082	-.120	-.143			
	.741	-.186	-.180	-.152	-----	.041	-.077	-.162	-.180	-.194			
	.852	-.167	-.144	-.093	.013	.034	-.025	-.102	-.140	-.161			
	.963	-.142	-.086	-.025	.016	.034	.011	-.040	-.094	-.137			
	.889	-.063	-.017	.032	.070	.101	.136	.172	.213	.259			
30	.926	-.048	.015	.044	.076	.096	.118	.149	.187	.234			
	.963	-.025	.016	.044	.068	.085	.109	.140	.178	.224			
	.111	-.086	-.028	-.003	.024	.036	.064	.076	.098	.126			
	.222	-.110	-.054	-.020	.004	.018	.036	.055	.075	.109			
	.333	-.143	-.025	.016	-.006	.001	.017	.035	.057	.083			
45	.444	-.170	-.038	-.020	.011	-.003	.006	.022	.038	.061			
	.555	-.185	-.062	-.023	-.009	.002	.008	.020	.034	.062			
	.666	-.190	-.074	-.030	-.019	.015	-.002	.016	.029	.052			
	.778	-.164	-.086	-.034	-.012	.006	0	.006	.019	.039			
	.889	-.048	.017	.057	.088	.122	.159	.201	.251	.303			
60	.926	-.132	-.048	.065	.093	.127	.165	.191	.234	.285			
	.963	-.141	-.044	.043	.074	.104	.132	.169	.214	.262			
	.889	-.057	-.024	.047	.074	.100	.128	.163	.203	.249			
	.926	-.040	.078	.081	.107	.134	.161	.199	.250	.302			
	.963	-.065	.033	.065	.083	.114	.146	.185	.233	.280			
180	.963	-.096	.043	.065	.073	.086	.123	.161	.204	.246			
	.083	.001	.028	.064	.072	.086	.063	.055	.036	.010			
	.204	-----	-.006	.011	.019	.026	.022	.014	-.008	-.027			
	.315	-.034	-.016	.004	.013	.014	.017	-.005	-.018	-.041			
	.426	-.063	-.033	-.018	-.001	.002	.009	.014	.032	.054			
	.537	-.061	-.039	-.021	-.016	.008	-.010	.017	.040	.065			
	.648	-.069	-.045	-.023	-.006	.008	-.010	.020	.044	.071			
	.759	-----	-----	-----	-----	-----	-----	-----	-----	-----			
	.870	-.065	-.039	-.019	-.007	.004	-.008	.016	.028	.049			
	.988	-.058	-.037	.019	-.004	.001	-.004	.019	.043	.072			
225	.130	.084	.087	.080	.062	.042	.018	-.005	-.027	-.065			
	.241	.060	.062	.040	.036	.020	.004	-.023	-.053	-.068			
	.352	.041	.038	.034	.025	.020	-.011	-.033	-.054	-.067			
	.463	-----	-----	-----	-----	-----	-----	-----	-----	-----			
	.574	.016	.006	.006	.005	.002	-.013	-.031	-.050	-.061			
	.685	.001	.001	.006	.002	-.010	-.023	-.043	-.056	-.063			
	.796	.017	.024	.028	.028	.011	-.008	-.030	-.048	-.059			
	.908	-.023	-.014	-.004	.006	.008	.005	.005	-.024	-.039			
	.148	.146	.124	.086	.048	.025	.009	-.006	-.010	-.033			
	.259	.137	.083	.047	.025	.003	-.009	-.017	-.026	-.041			
270	.370	.125	.086	.049	.024	.010	-.007	-.009	-.022	-.034			
	.481	.103	.061	.036	.013	.007	-.014	.020	.030	.046			
	.592	.085	.057	.024	.003	.013	-.015	.023	.032	.050			
	.704	.078	.041	.018	0	.014	-.018	-.024	-.039	-.052			
	.815	.072	.039	.014	-.002	-.018	-.021	-.026	-.031	-.042			
	.926	.263	.216	.170	.134	.096	.072	.056	.031	.083			
	.862	.256	.231	.209	.175	.130	.112	.086	.097	.072			
	.815	.252	.233	.203	.169	.132	.093	.070	.042	-.035			
	.768	.245	.224	.175	.137	.099	.065	.013	-.046	-.076			
	.720	.237	.194	.152	.117	.080	.048	-.008	-.048	-.091			
350	.778	.209	.178	.142	.113	.064	.011	-.034	-.091	-.142			
	.815	.213	.174	.136	.097	.058	.019	-.016	-.125	-.221			
	.862	.196	.160	.122	.080	.058	.028	0	-.188	-.289			
	.915	.183	.160	.128	.093	.048	.001	-.135	-.224	-.237			
	.963	-.183	.146	.119	.091	.068	.017	-.158	-.230	-.218			

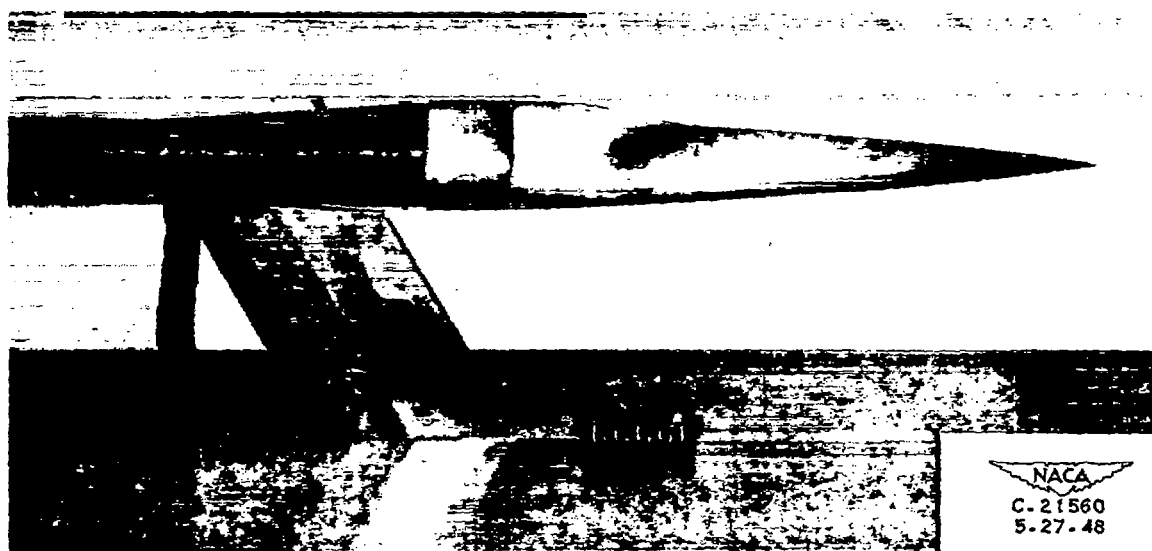
TABLE IV - TABULATED PRESSURE COEFFICIENTS AT 5° ANGLE OF ATTACK FOR RANGE OF YAW ANGLES

Angle of yaw, γ deg	x/l	12	9	6	3	0	-3	-6	-9	-12
		Pressure coefficient, C_p								
0	.074	-.115	-.066	-.017	.027	.033	.014	-.014	-.057	-.102
	.185	-.111	-.070	-.028	.006	.015	.001	-.028	-.061	-.095
	.296	-.102	-.071	-.038	-.004	.012	.002	-.024	-.052	-.079
	.408	-.106	-.066	-.036	-.004	.008	.001	-.017	-.045	-.082
	.518	-.096	-.062	-.033	-.009	.008	.001	-.020	-.052	-.082
	.630	-.088	-.054	-.027	-.008	.004	-.014	-.030	-.054	-.088
	.741	-.133	-.103	-.075	-.019	.056	-.027	-.051	-.079	-.111
	.852	-.111	-.082	-.042	.008	.051	.010	-.019	-.053	-.086
	.963	-.108	-.052	-.003	.030	.052	.037	.009	-.041	-.096
30	.889	-.050	-.017	.070	.103	.128	.148	.183	.213	.249
	.926	-.084	-.021	.058	.088	.110	.131	.167	.197	.232
	.963	-.089	-.013	.058	.078	.096	.107	.137	.164	.197
45	.111	-.047	-.020	.006	.020	.026	.028	.044	.065	.077
	.222	-.063	-.018	.001	.012	.020	.028	.039	.058	.086
	.333	-.073	-.011	-.002	.003	.010	.015	.022	.033	.056
	.444	-.093	-.029	-.007	.004	.004	.002	.010	.021	.032
	.555	-.100	-.031	-.008	.005	.004	.006	.012	.020	.033
	.666	-.094	-.041	-.014	-.005	.002	.006	.011	.017	.032
	.778	-.082	-.039	-.005	.007	.010	.003	.003	.007	.018
	.852	.034	.106	.119	.121	.151	.177	.211	.242	.287
	.889	.044	.087	.112	.117	.138	.160	.197	.228	.273
	.926	-.012	.044	.083	.097	.121	.145	.181	.213	.250
	.963	-.039	.041	.068	.079	.102	.123	.159	.194	.231
60	.999	.102	.128	.118	.117	.147	.169	.202	.230	.274
	.926	.085	.086	.086	.096	.122	.145	.180	.210	.248
	.963	.051	.049	.067	.081	.109	.134	.172	.211	.251
180	.093	.083	.103	.124	.136	.126	.115	.112	.093	.069
	.204	.036	.062	.084	.093	.102	.102	.097	.087	.077
	.315	.046	.066	.063	.072	.080	.077	.076	.071	.051
	.426	.021		.048	.055	.056	.059	.067	.070	.027
	.537	.008	.021	.037	.052	.065	.059	.057	.042	.026
	.648	.008	.027	.044	.048	.059	.058	.055	.042	.025
	.759	-.012	.012	.027	.038	.046	.047	.049	.036	.019
	.870	-----	-----	-----	-----	-----	-----	-----	-----	-----
	.982	.024	.039	.051	.051	.058	.060	.060	.040	.003
225	.130	.178	.167	.149	.113	.073	.037	.001	.041	.085
	.241	-----	-----	-----	-----	-----	-----	-----	-----	-----
	.352	.153	.122	.096	.092	.037	.002	.030	.080	.089
	.463	.127	.105	.083	.056	.026	.009	.047	.084	.083
	.574	.122	.101	.083	.061	.031	.004	.042	.091	.119
	.685	.123	.093	.077	.051	.020	.016	.057	.109	.137
	.796	.070	.069	.067	.043	.015	.022	.065	.113	.124
	.908	.149	.141	.124	.103	.072	.029	.009	-.049	.067
270	.148	.118	.090	.067	.031	.011	.002	.017	-.048	.063
	.259	.102	.064	.025	.007		.008	.033	-.042	.068
	.370	.111	.065	.030	.017	.006	.013	.012	-.029	.053
	.491	.083	.046	.025	.005	.002	.003	.018	-.042	.053
	.592	.076	.039	.018	.004	.005	.004	.016	-.028	.053
	.704	.067	.032	.006	.007	.010	.005	.011	-.026	.058
	.815	.057	.026	.007	.005	.010	.007	.014	-.027	.069
	.926	.218	.184	.163	.138	.118	.102	.088	.048	.041
300	.852	.194	.194	.203	.189	.165	.152	.161	.132	.072
315	.852	.306	.262	.223	.186	.154	.148	.157	.153	.063
330	.862	.269	.228	.187	.153	.124	.116	.093	.045	.004
340	.815	.235	.199	.159	.128	.098	.079	.054	.023	.024
	.552	.227	.185	.151	.122	.099	.088	.042	-.005	.053
350	.778	.201	.169	.135	.107	.076	.042	.025	-.011	.046
	.915	.195	.161	.130	.104	.080	.049	.019	-.028	.083
	.852	.170	.135	.108	.087	.076	.063	.026	-.054	.118
355	.778	.166	.141	.114	.093	.066	.031	.020	-.101	.148
	.815	.149	.124	.104	.086	.067	.038	.055	-.102	.143

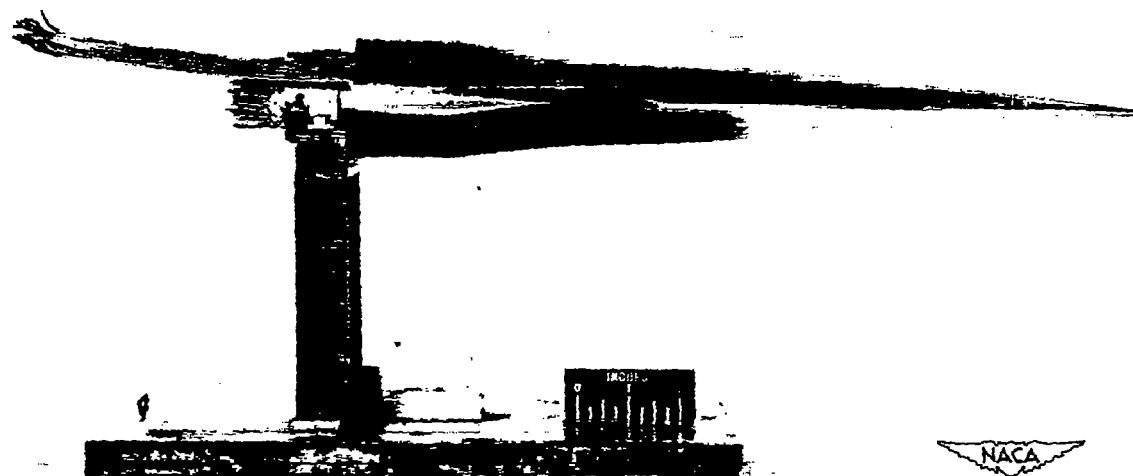
TABLE V - TABULATED PRESSURE COEFFICIENTS AT 10° ANGLE OF ATTACK
FOR RANGE OF YAW ANGLES

Angle of yaw, γ deg		12	9	6	3	0	-3	-6	-9	-10
θ (deg)	x/L	Pressure coefficient, C_p								
0	.074	-.123	-.088	-.051	-.012	.012	-.015	-.036	-.073	-.112
	.185	-.110	-.080	-.044	-.026	.012	-.035	-.046	-.072	-.101
	.296	-.088	-.046	-.046	-.030	.018	-.032	-.053	-.077	-.104
	.406	-.102	-.077	-.048	-.025	.015	-.032	-.043	-.065	-.097
	.516	-.100	-.072	-.045	-.018	.012	-.021	-.030	-.060	-.086
	.630	-.100	-.068	-.038	-.029	.024	-.027	-.043	-.070	-.104
	.741	-.101	-.084	-.032	-.011	.026	-.007	-.038	-.081	-.114
	.852	-.101	-.090	-.047		.014	0	-.049	-.082	-.112
	.963	-.101	-.097	-.042		.006	-.006	-.053	-.108	-.139
	30	.889	-.000	.025	.042	.077	.076	.090	.121	.147
.926		-.000	.022	.069	.070	.064	.072	.097	.127	.156
.963		-.000	.024	.038	.060	.042	.067	.080	.103	.134
45	.111	-.000	.055	-.038	-.021	-.022	-.028	-.021	-.017	-.016
	.222	-.000	.055	-.038	-.021	-.022	-.028	-.021	-.017	-.016
	.333	-.000	.064	-.030	-.029	.046	-.045	-.045	-.045	-.014
	.444	-.000	.061	-.043	-.031	.038	-.051	-.053	-.053	-.045
	.555	-.081	-.062	-.041	-.040	.032	-.038	-.047	-.049	-.039
	.666	-.082	-.067	-.049	-.059	.044	-.044	-.053	-.060	-.048
	.778	-.088	-.056	-.041	-.052	.022	-.039	-.065	-.070	-.057
	.852	-.067	-.066	.073	-.059	.100	.120	.141	.161	.150
	.889	-.068	-.059	.056	-.063	.080	.099	.124	.142	.163
	.926	-.057	-.068	.059	-.040	.066	.083	.113	.143	.171
60	.963	-.051	-.038	.034	-.028	.052	.069	.094	.126	.157
	.889	-.050	.022	.029	.022	.090	.104	.123	.127	.128
	.926	-.048	-.010	-.037	.002	.067	.086	.109	.130	.147
180	.963	-.000	.139	-.037	.011	.054	.076	.104	.137	.167
	.093	.165	.169	.181	.206	.204	.188	.187	.167	.155
	.204	.106	.116	.143	.148	.148	.141	.143	.141	.127
	.316	.101	.113	.118	.120	.126	.124	.129	.134	.127
	.426	.090	.089	.091	.097	.105	.105	.097	.095	.089
	.537	.061	.066	.077	.088	.098	.109	.116	.098	.093
	.648	.056	.062	.074	.081	.089	.090	.072	.063	.061
	.759	.039	.053	.056	.058	.068	.067	.067	.062	.057
	.870	.044	.052	.061	.072	.077	.075	.065	.059	.054
	.982	.083	.090	.102	.112	.116	.116	.108	.102	.088
225	.130	.257	.211	.175	.139	.078	.017	-.035	-.083	-.136
	.241	.208	.195	.148	.094	.034	-.024	-.082	-.135	.175
	.352	.220	.175	.122	.060	.024	-.031	-.094	-.152	.191
	.463	.187	.141	.091	.046	.004	-.057	-.107	-.162	.183
	.574	.172	.133	.088	.040	.007	-.063	-.114	-.173	.206
	.685	.157	.119	.085	.024	.026	-.081	-.133	-.197	.221
	.796	.143	.096	.080	.013	.034	-.089	-.148	-.207	.202
	.908	.161	.129	.091	.049	.006	-.061	-.133	-.161	.138
270	.148	.083	.014	-.001	-.036	.056	-.067	-.102	-.145	.167
	.259	.006	-.015	-.054	-.076	.074	-.097	-.125	-.167	.190
	.370	.036	-.012	-.051	-.062	.073	-.103	-.124	-.161	.170
	.481	.013	-.031	-.061	-.075	.083	-.104	-.137	-.140	.179
	.592	.003	-.042	-.067	-.084	.088	-.093	-.122	-.140	.162
	.704	.023	-.057	-.076	-.089	.097	-.102	-.104	-.125	.146
	.816	.031	-.066	-.084	-.088	.082	-.091	-.099	-.119	.174
	.926	.103	.061	.039	.051	.052	.013	-.014	-.065	.202
300	.852	.074	.075	.118	.125	.090	.026	.031	.039	.017
	.315	.852	.200	.189	.166	.135	.100	.109	.089	.087
	.330	.852	.200	.170	.142	.110	.092	.082	.063	.047
340	.815	.159	.144	.114	.081	.064	.068	-.040	I----	.022
	.852	.168	.139	.114	.083	.067	.055	-.025	m	.052
350	.778	.124	.109	.086	.050	.041	.036	.004	.028	.051
	.815	.134	.116	.088	.063	.054	.042	-.005	.038	.087
	.852	.118	.089	.061	.042	.040	.017	-.022	.082	.125
355	.778	.105	.087	.068	.039	.042	.024	-.022	.072	.102
	.816	.087	.078	.063	.044	.044	.020	-.039	.095	.130

1025



(a) Side view showing method of support .

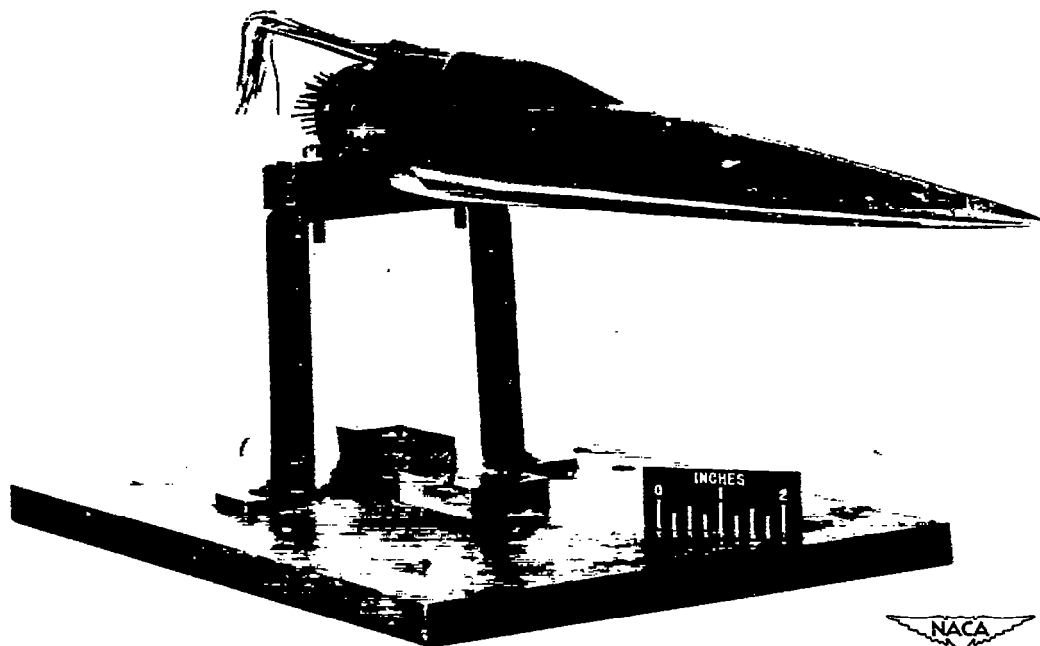


(b) Top view.

Figure 1. - Photographs of model used in investigation.

1000

1000



NACA
C-21761
7-6-48

(c) Three-quarter front view.



NACA
C-21561
5-27-48

(d) Three-quarter close-up rear view.

Figure 1. - Concluded. Photographs of model used in investigation.

1875

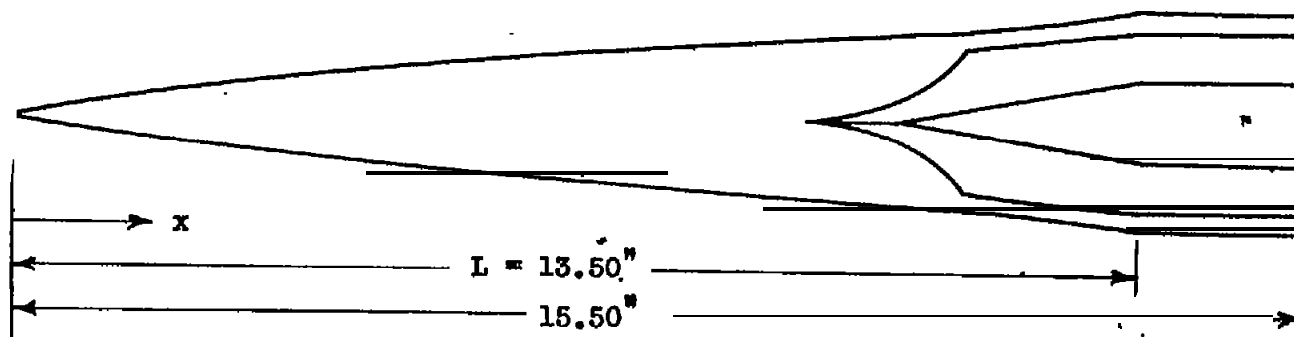
1

2

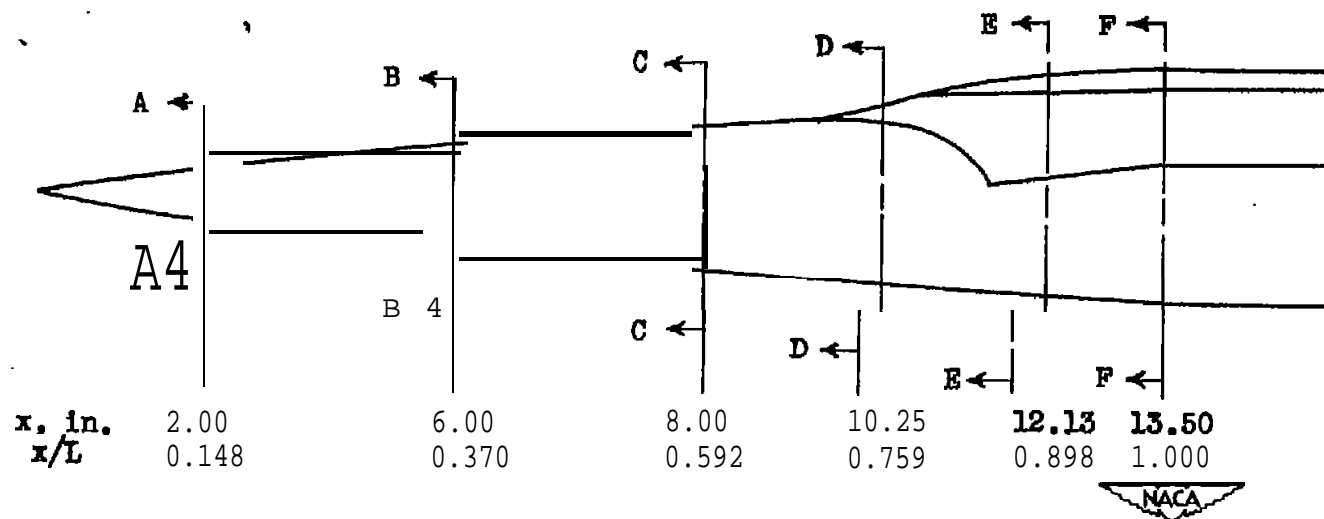
3

4

1876

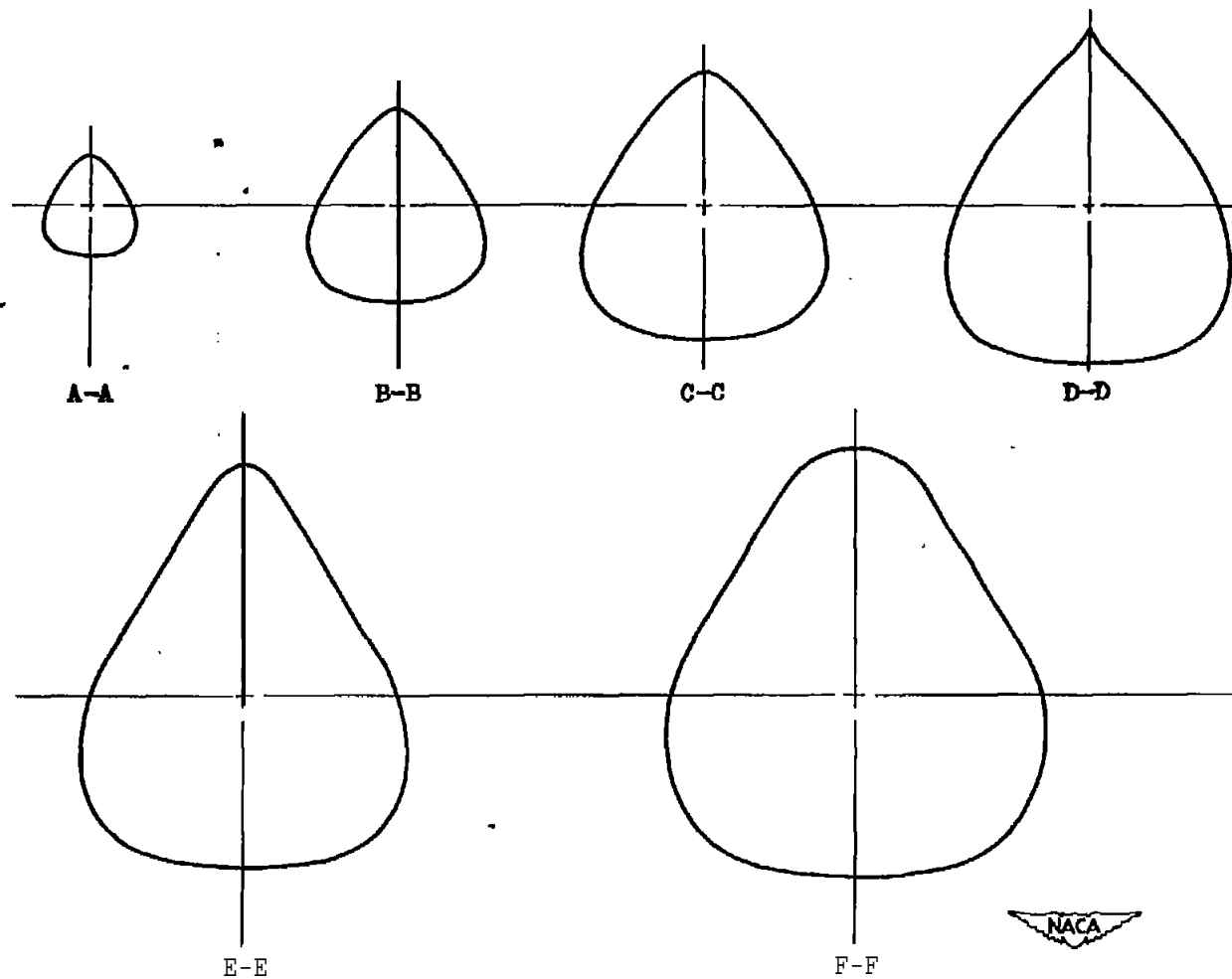


(a) Top view, half size.



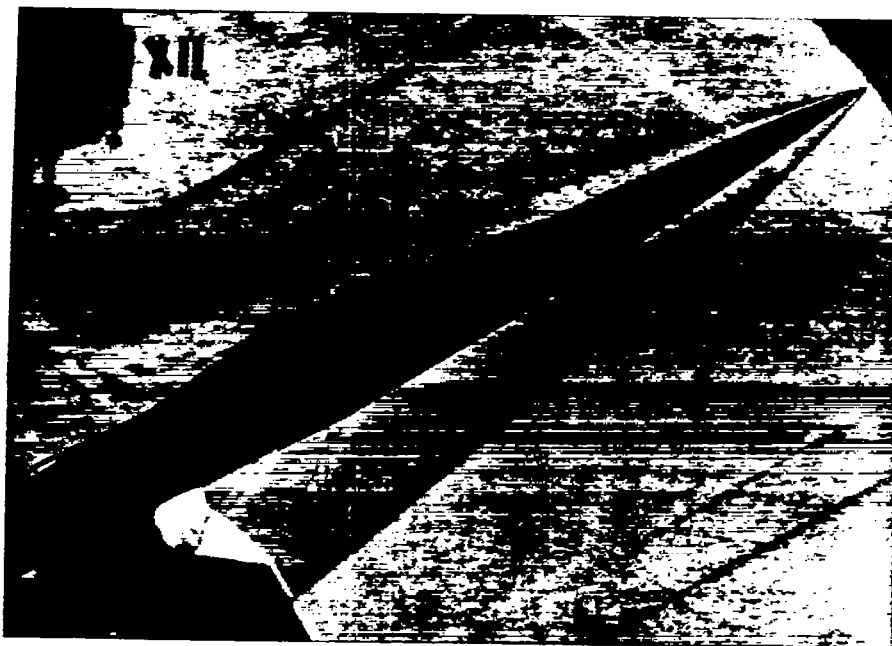
(b) Side view, half size.

Figure 2. - Sketch of model showing principal dimensions and typical cross sections.

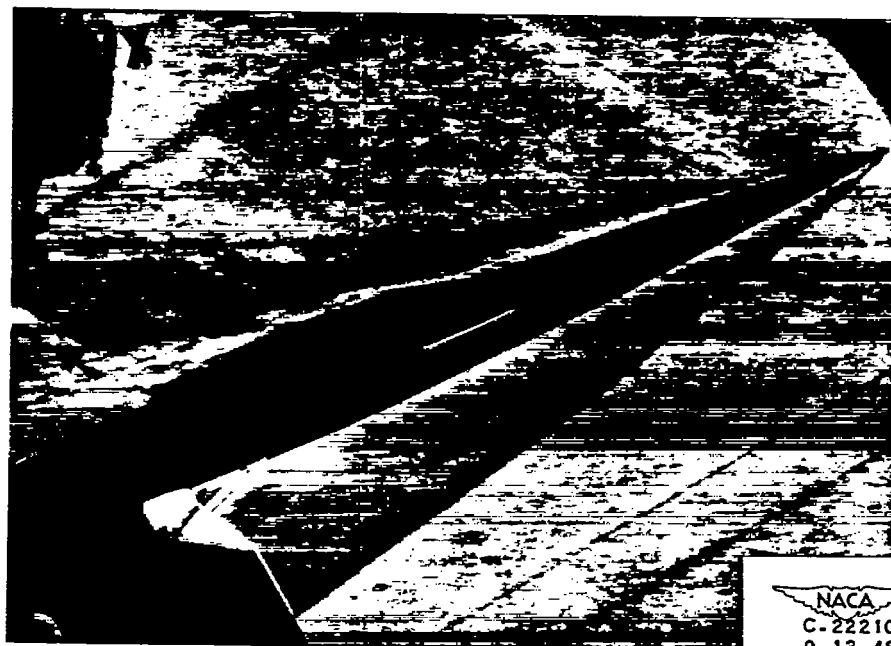


(a) Typical cross sections, full size (fig. 2(b)).

Figure 2. - Concluded. Sketch of model, showing principal dimensions and typical cross sections.



(a) Angle of attack, 30° .



(b) Angle of attack, 24° .

Figure 3. - Schlieren photographs of model at 0° angle of yaw.

1910

1910



(c) Angle of attack, 18° .



(d) Angle of attack, 12° .

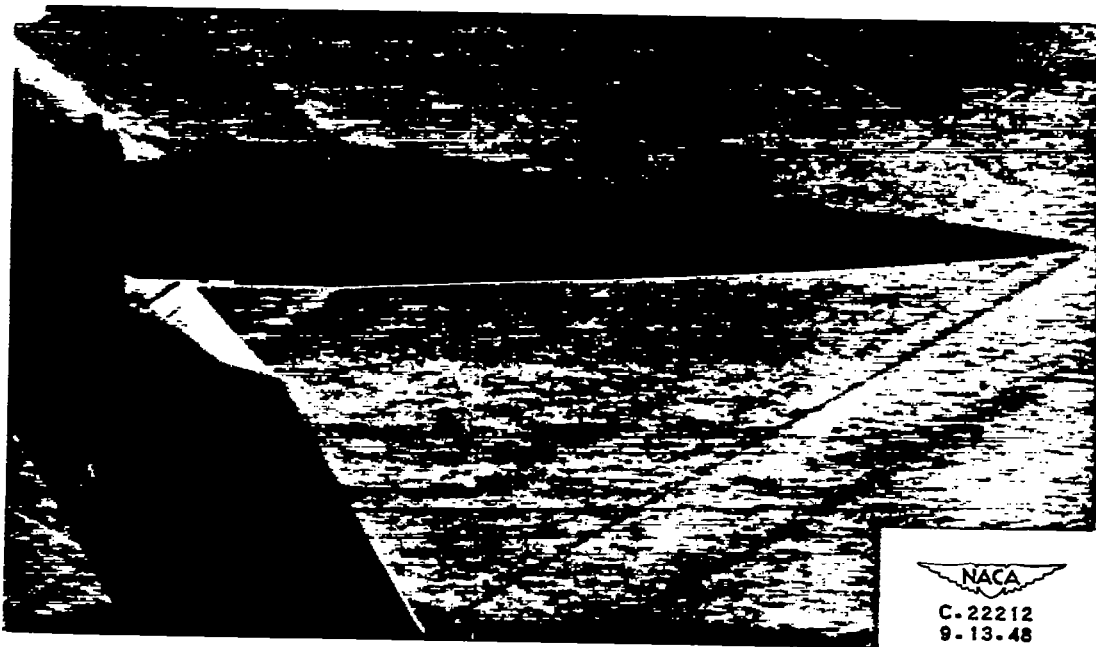
Figure 3. - Continued. Schlieren photographs of model at 0° angle of yaw.

1875

1875



(e) Angle of attack, 6° .



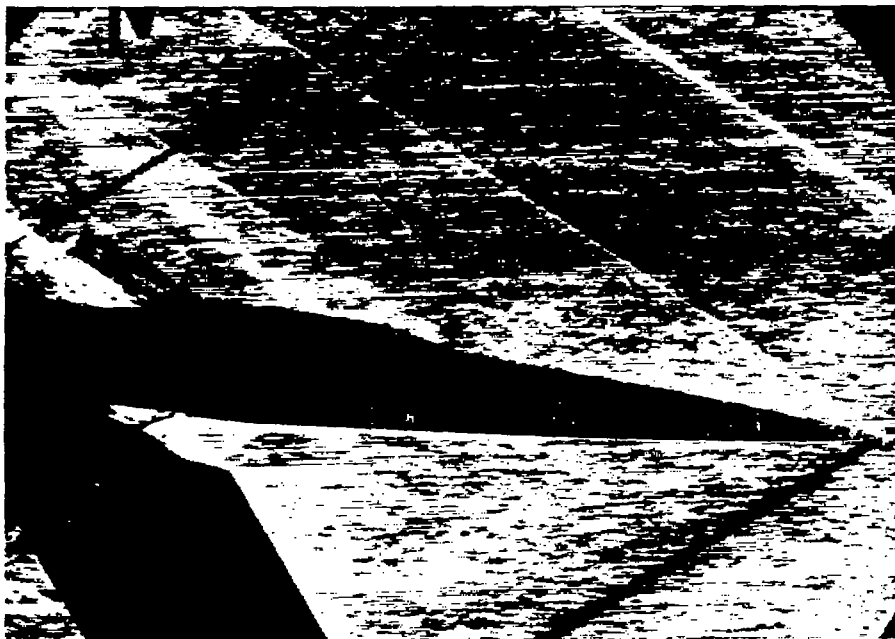
(f) Angle of attack, 0° .

Figure 3. - Continued. Schlieren photographs of model at 0° angle of yaw.

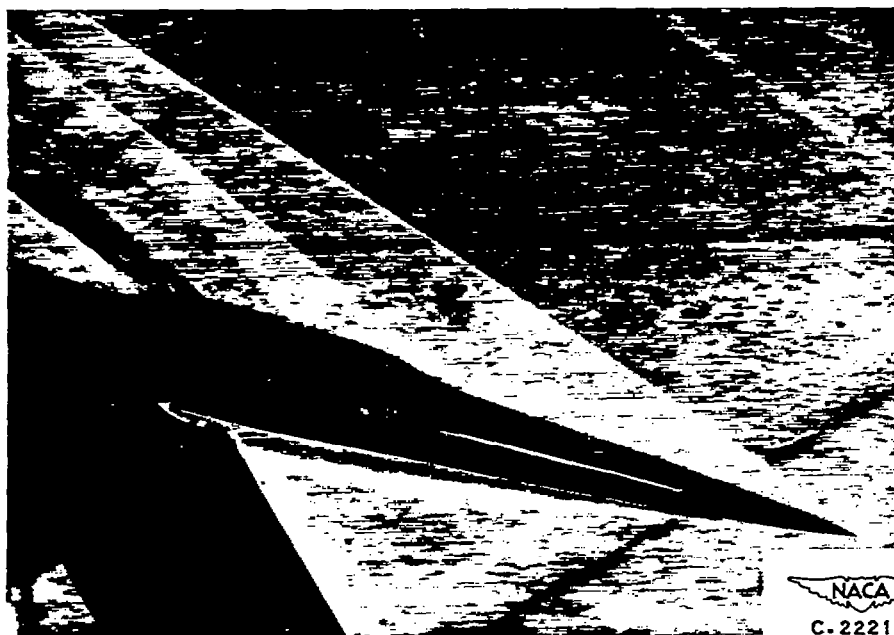
████████████████████

•
•

████████████████████



(g) Angle of attack, -6° .



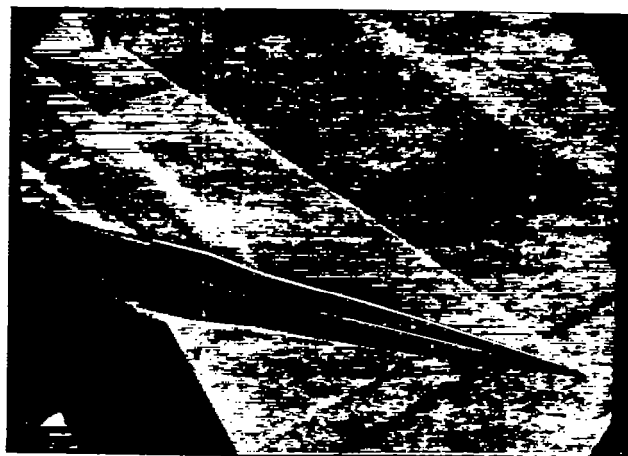
NACA
C. 22213
9-13-48

(h) Angle of attack, -15° .

Figure 3. - Concluded. Schlieren photographs of model at 0° angle of yaw.

1. The first part of the document is a list of names and addresses of the members of the committee.

2. The second part of the document is a list of names and addresses of the members of the committee.



(a) Angle of yaw, 12° .



(b) Angle of yaw, 6° .



(c) Angle of yaw, 0° .

Figure 4. - Schlieren photographs of model at 0° angle or attack.

1000

.

.

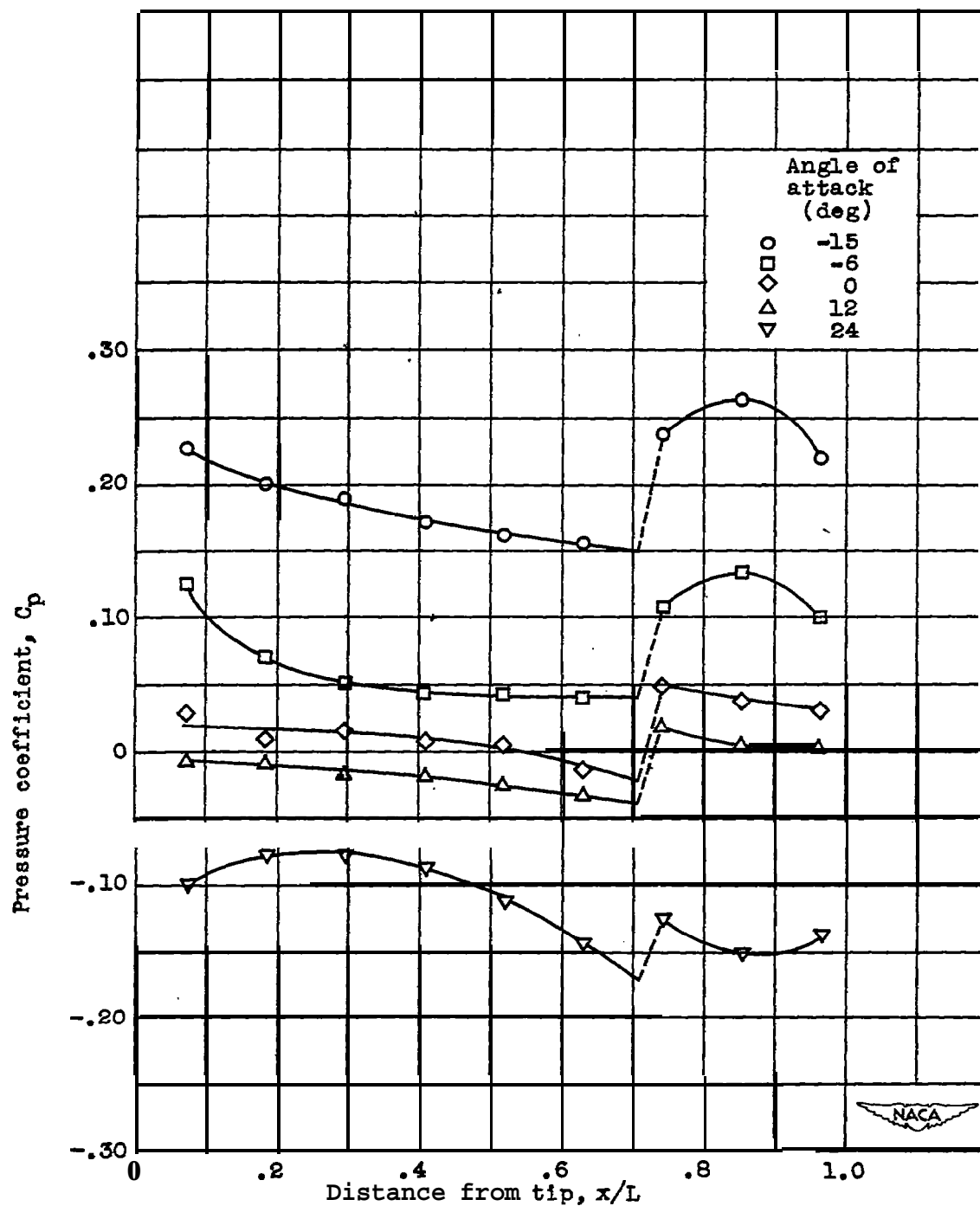
.

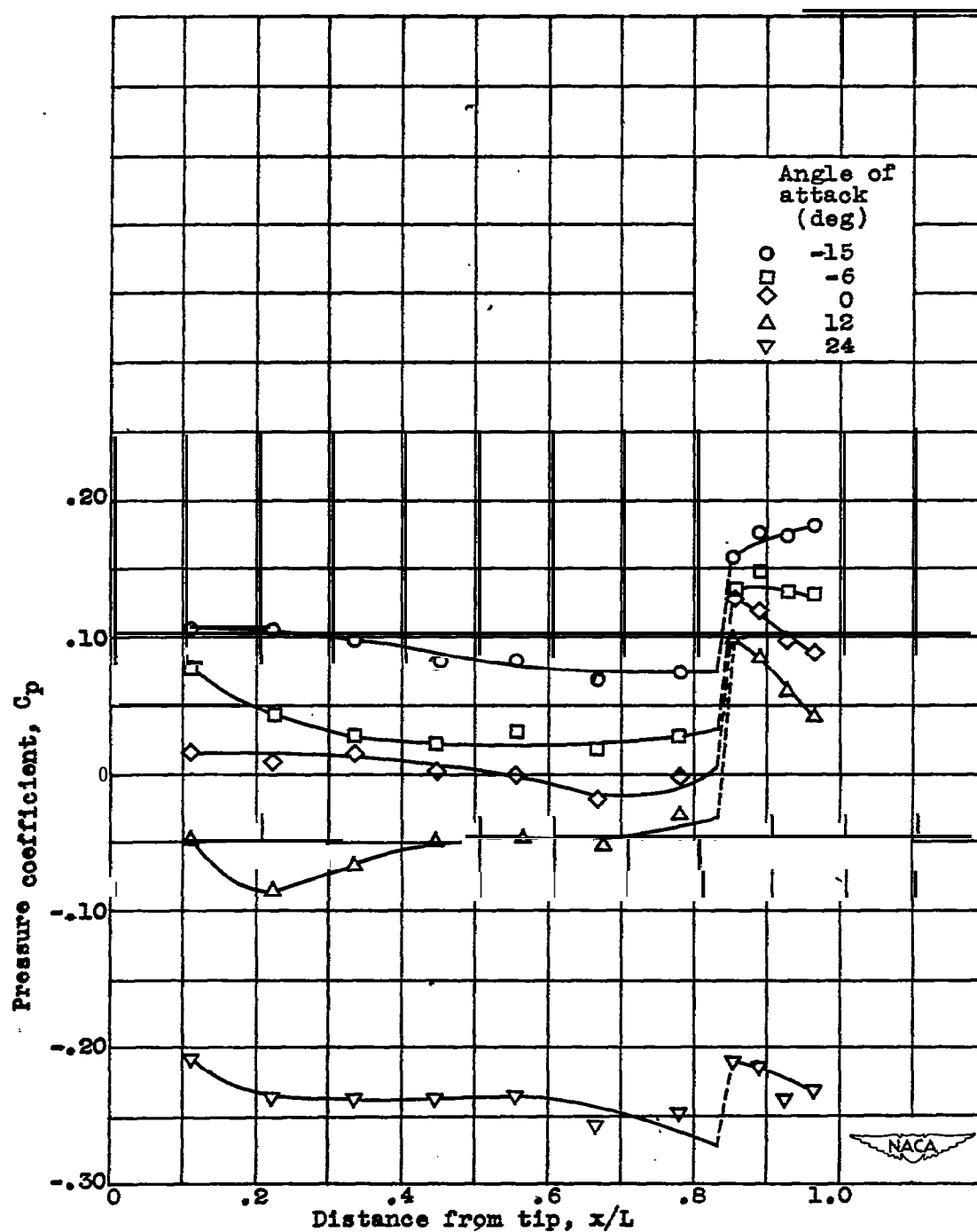
.

.

.

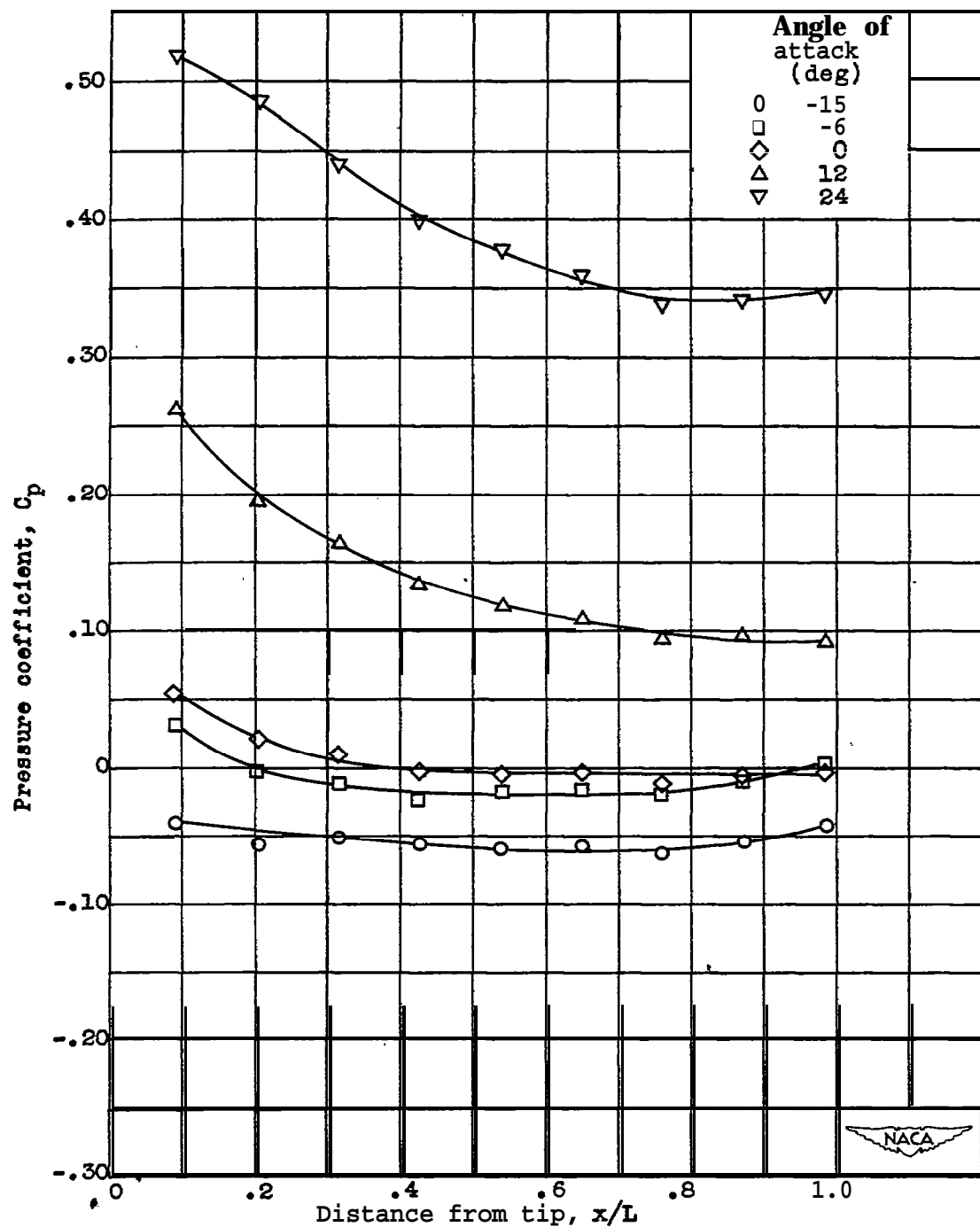
1000

(a) $\theta = 0^\circ$ longitudinal plane.Figure 5. - Pressure distributions along longitudinal planes at 0° yaw angle for range of angles of attack.



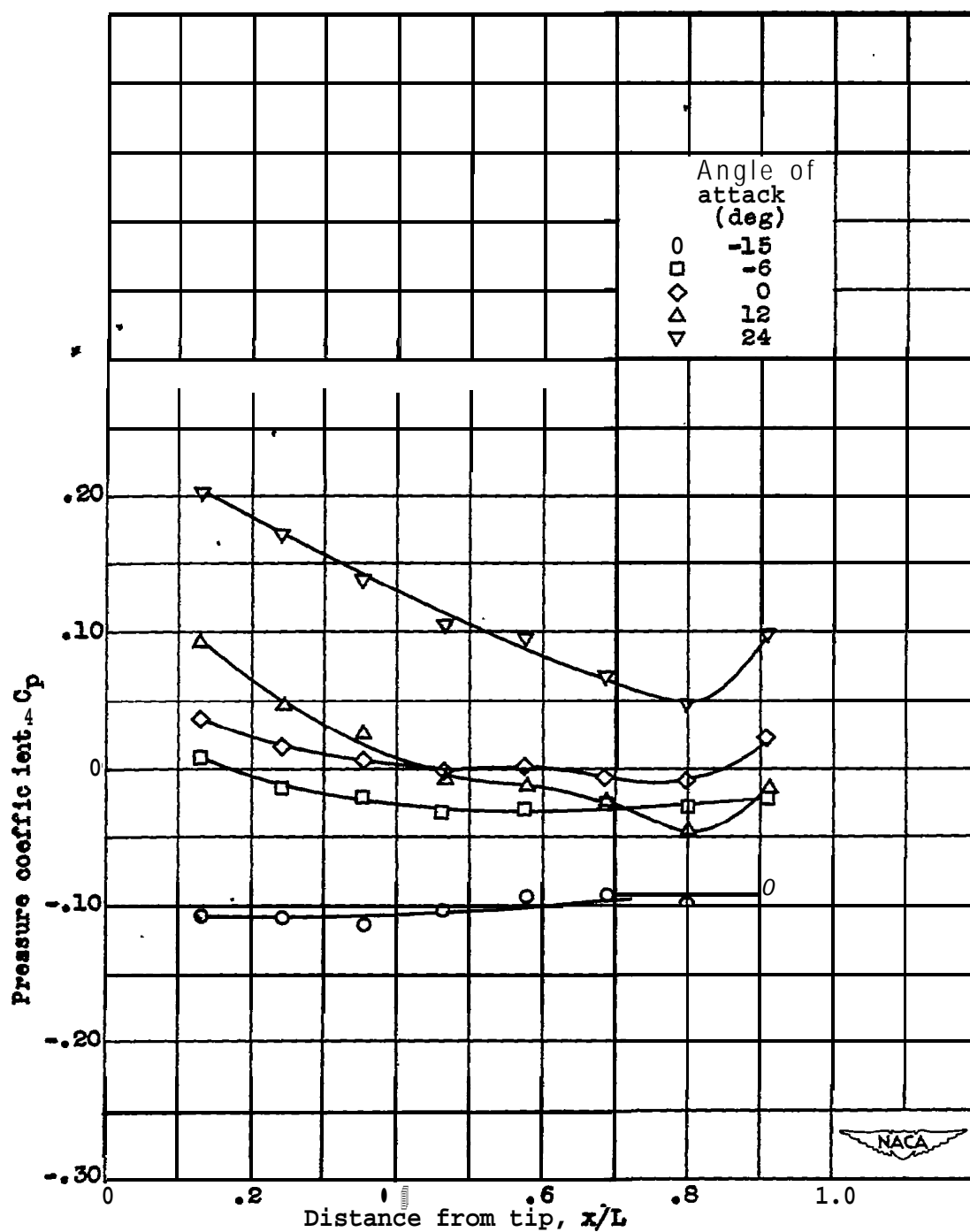
(b) $\theta = 45^\circ$ longitudinal plane.

Figure 5. - Continued. Pressure distributions along longitudinal planes at 0° yaw angle for range of angles of attack.



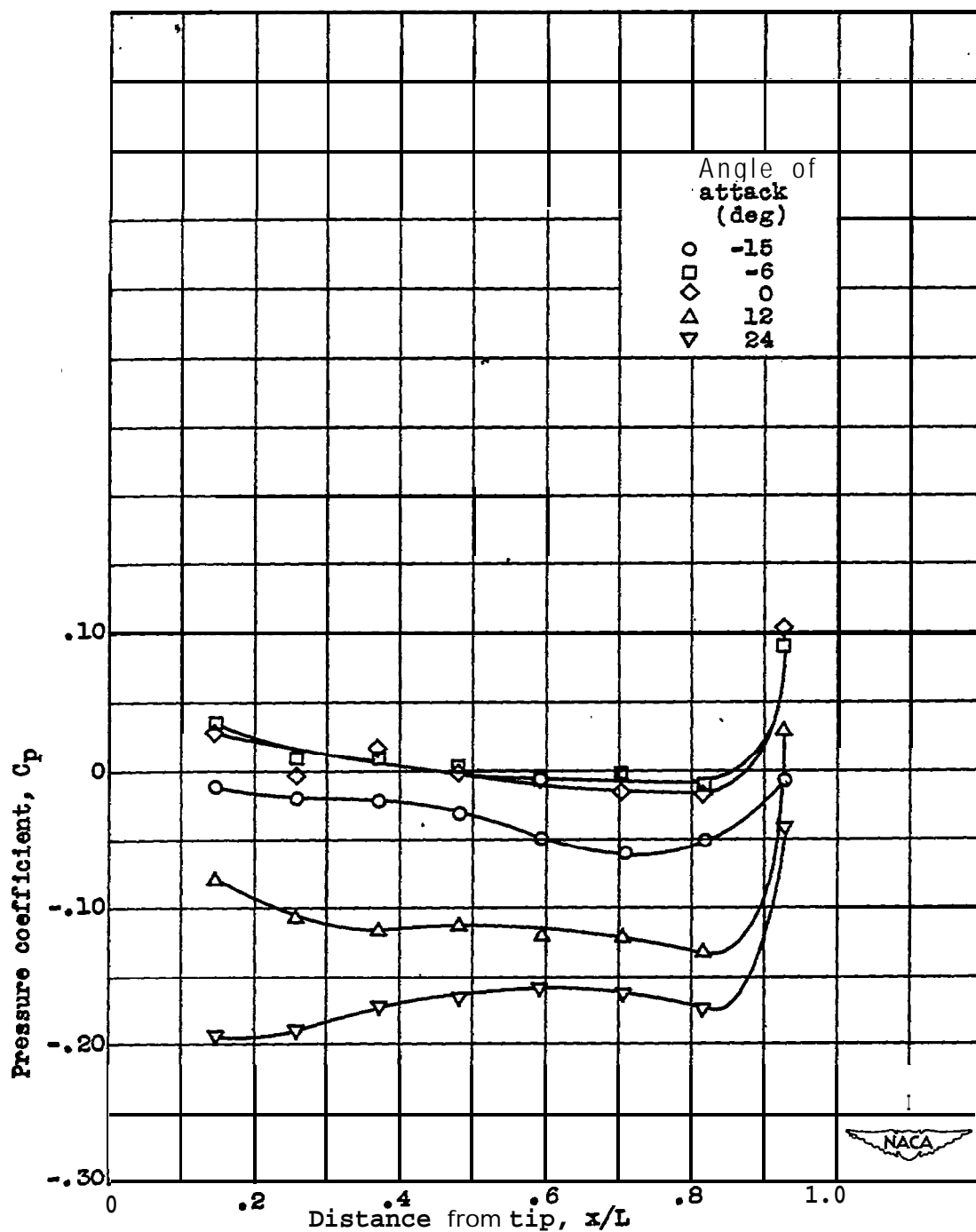
(c) $\theta = 180^\circ$ longitudinal plane. .

Figure 5. - Continued. Pressure distributions along longitudinal planes at 0° yaw angle for range of angles of attack.



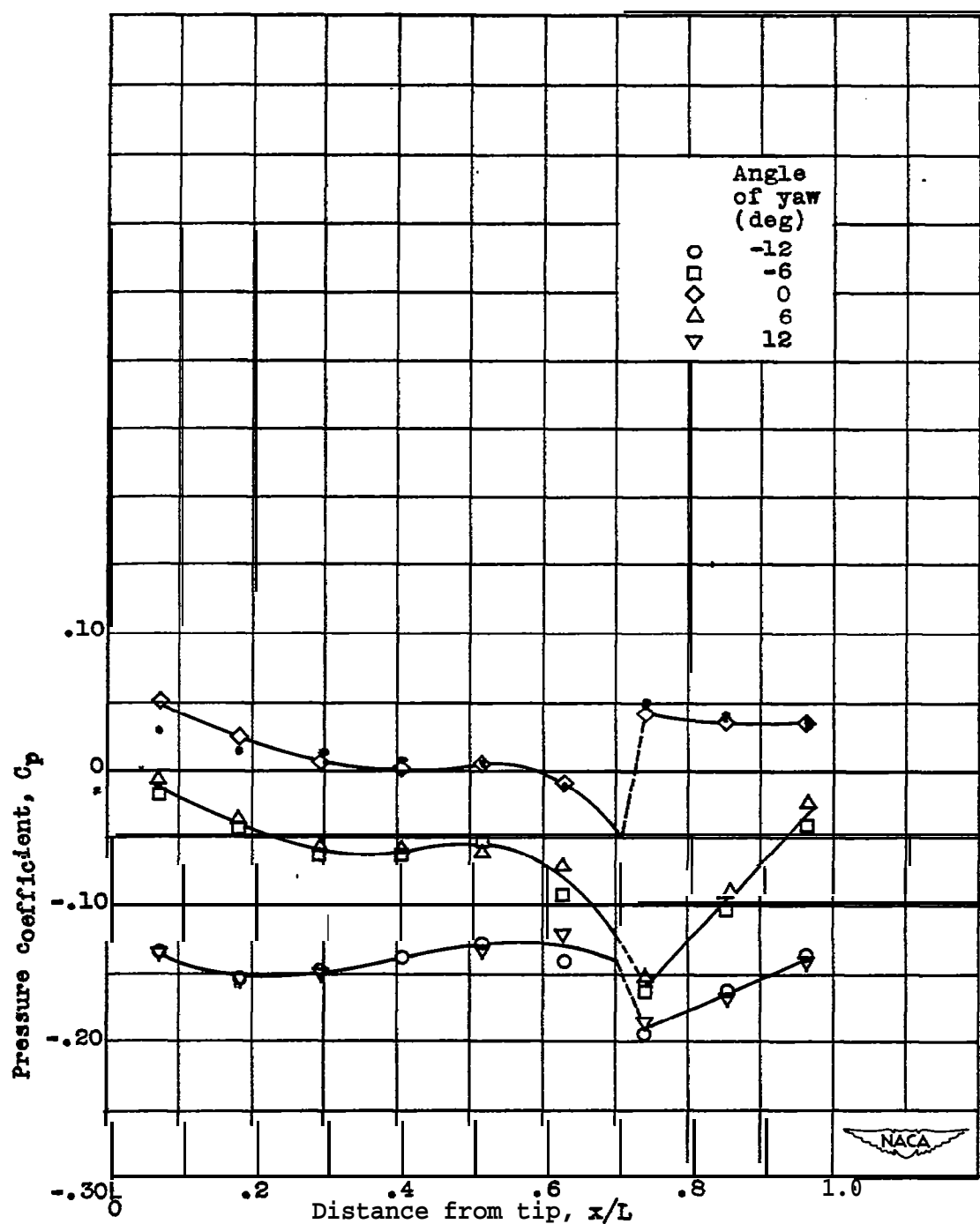
(d) $\theta = 225^\circ$ longitudinal plane.

Figure 5. - Continued. Pressure distributions along longitudinal planes at 0° yaw angle for range of angles of attack.



(e) $\theta = 270^\circ$ longitudinal plane.

Figure 5. - Concluded. Pressure distributions along longitudinal planes at 0° yaw angle for range of angles of attack.

(a) $\theta = 0^\circ$ longitudinal plane.Figure 6. - Pressure distributions along longitudinal planes at 0° angle of attack for range of yaw angles.

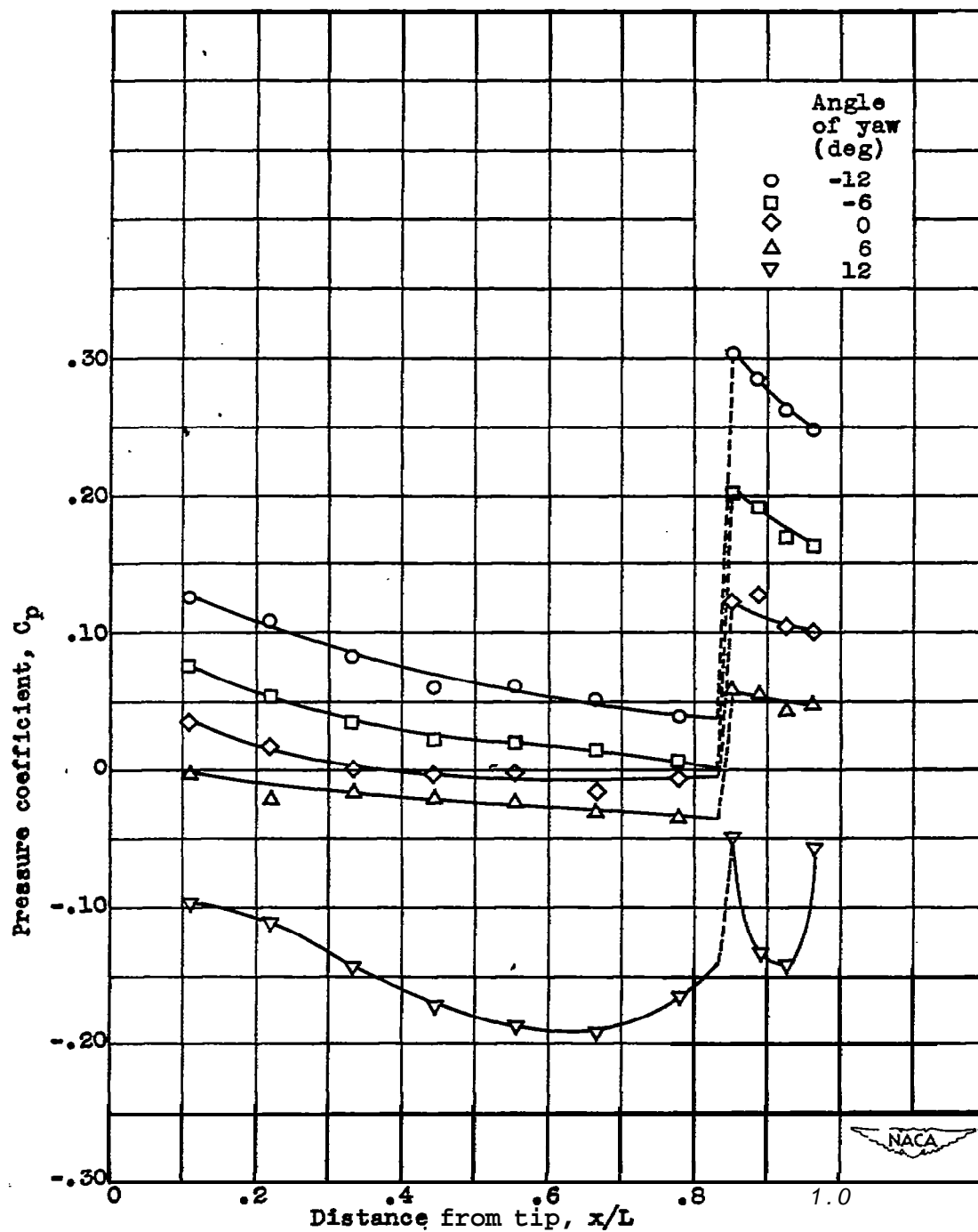
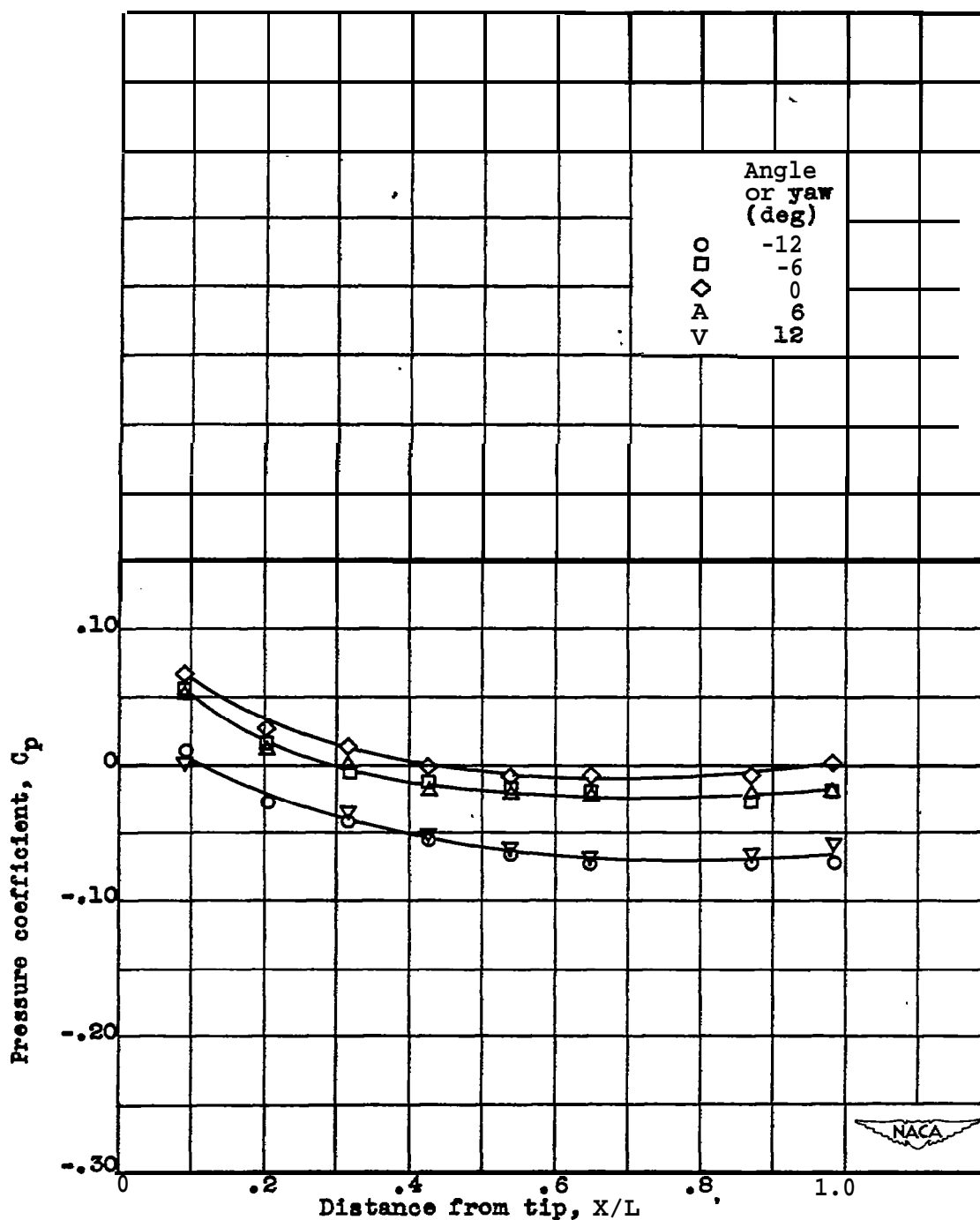
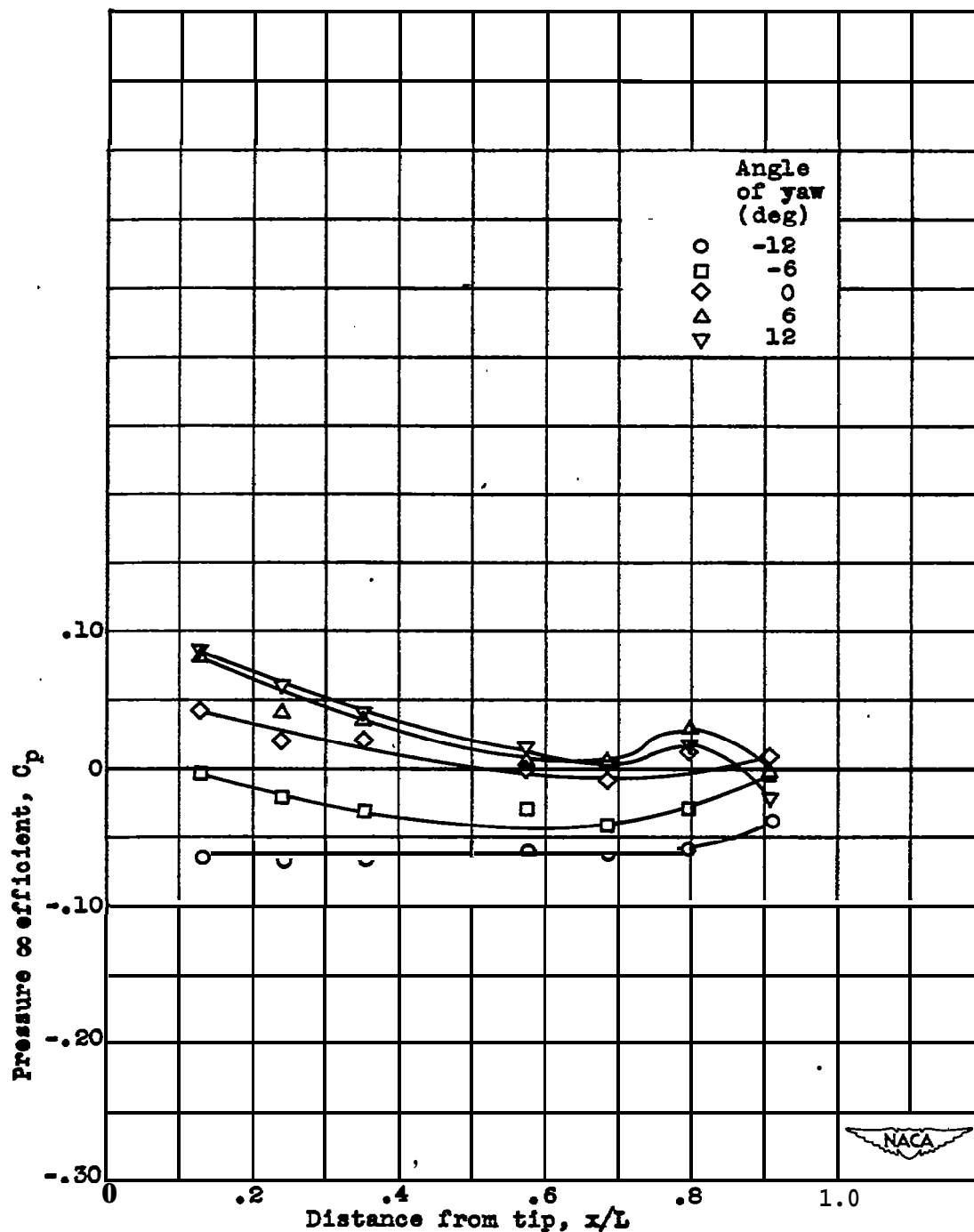


Figure 6. - Continued. Pressure distributions along longitudinal planes at 0° angle of attack for range of yaw angles.



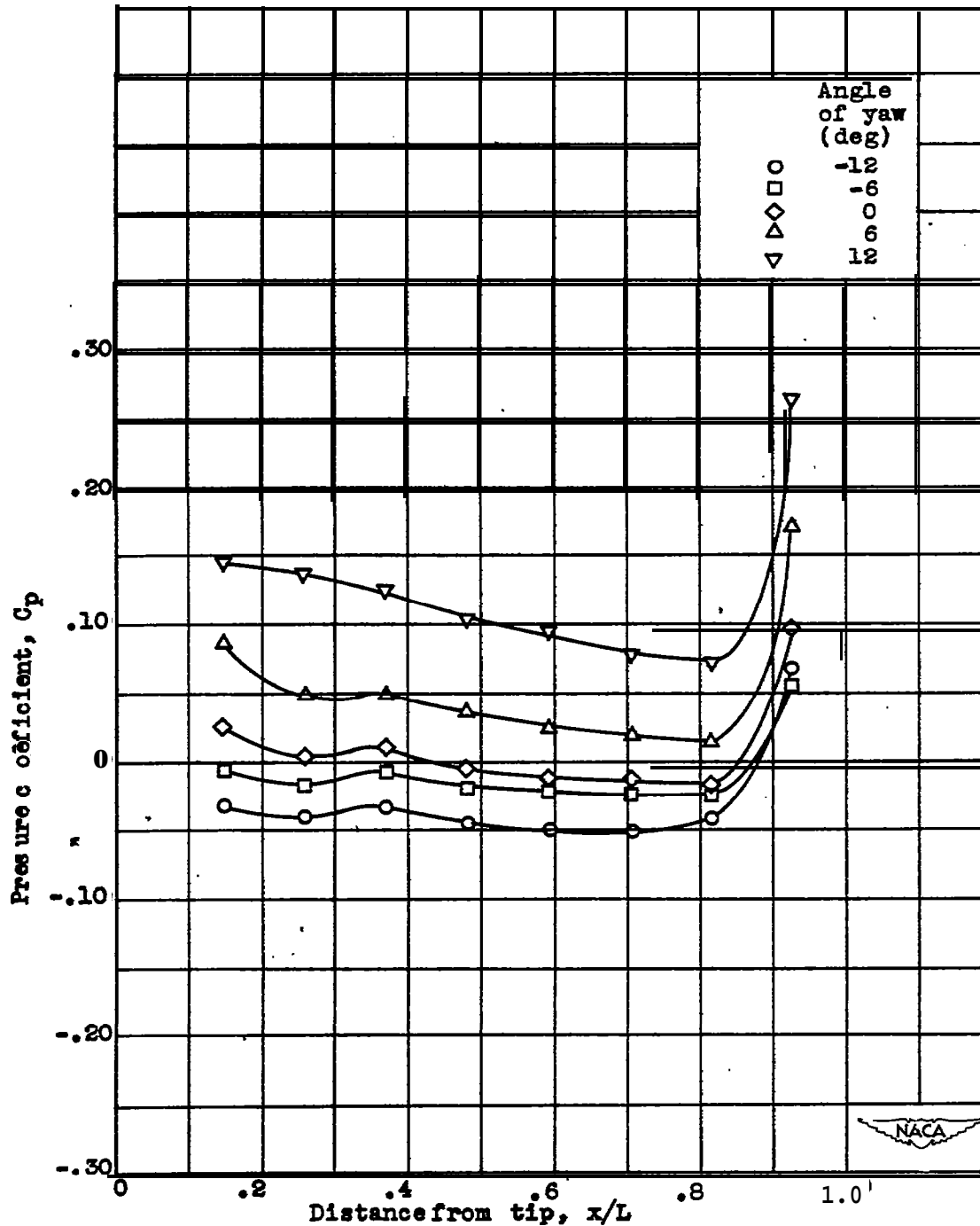
(c) $\theta = 180^\circ$ longitudinal plane.

Figure 6. - Continued. Pressure distributions along longitudinal planer at 0° angle of attack for range of yaw angles.



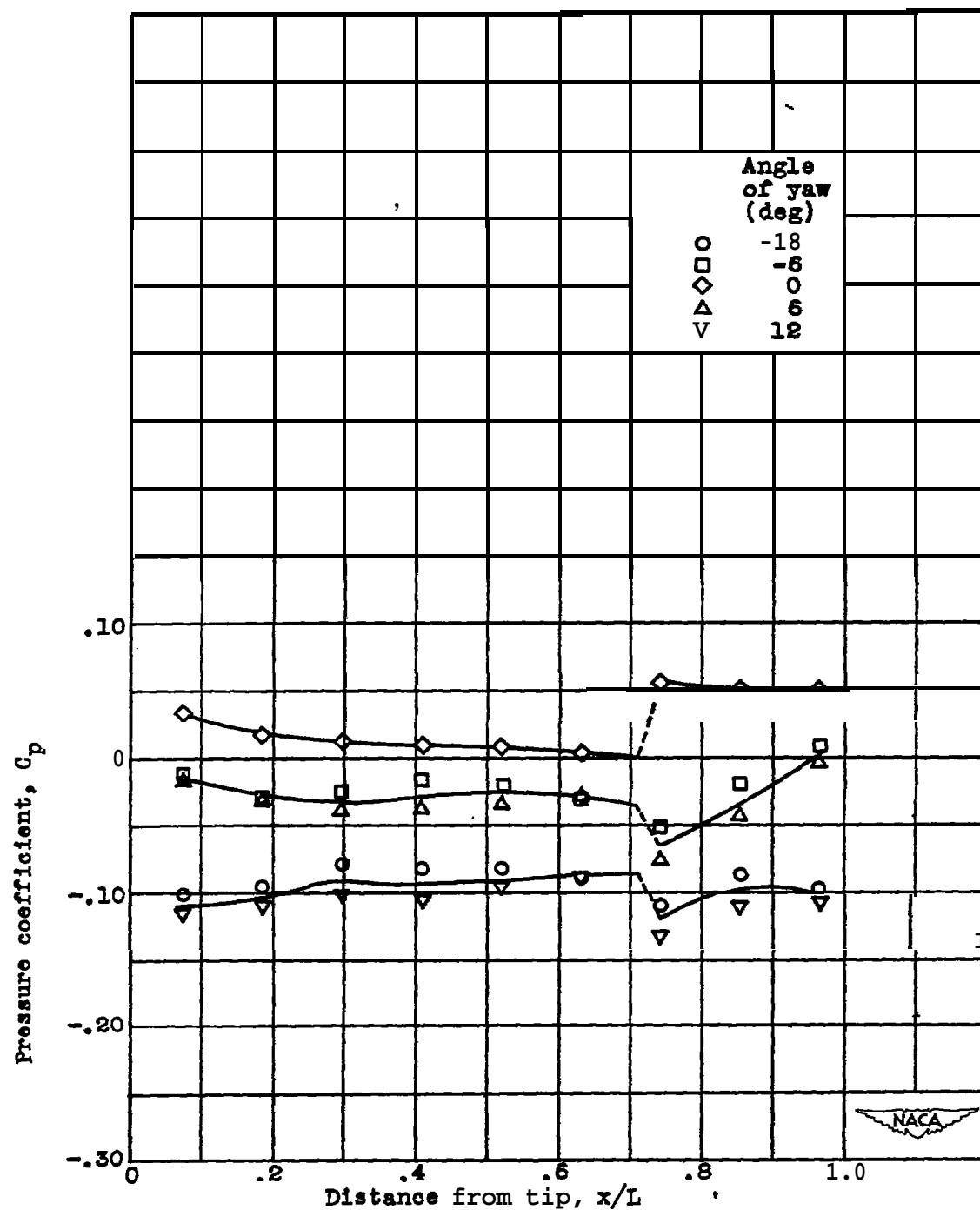
(d) $\theta = 225^\circ$ longitudinal plane.

Figure 6. - Continued. Pressure distributions along longitudinal planes at 0° angle of attack for range of yaw angles.



(e) $\theta = 270^\circ$ longitudinal plane.

Figure 6. - Concluded. Pressure distributions along longitudinal planes at 0° angle of attack for range of yaw angles.



(a) $\theta = 0^\circ$ longitudinal plane.

Figure 7. - Pressure distributions along longitudinal plane at 5° angle of attack for range of yaw angles.

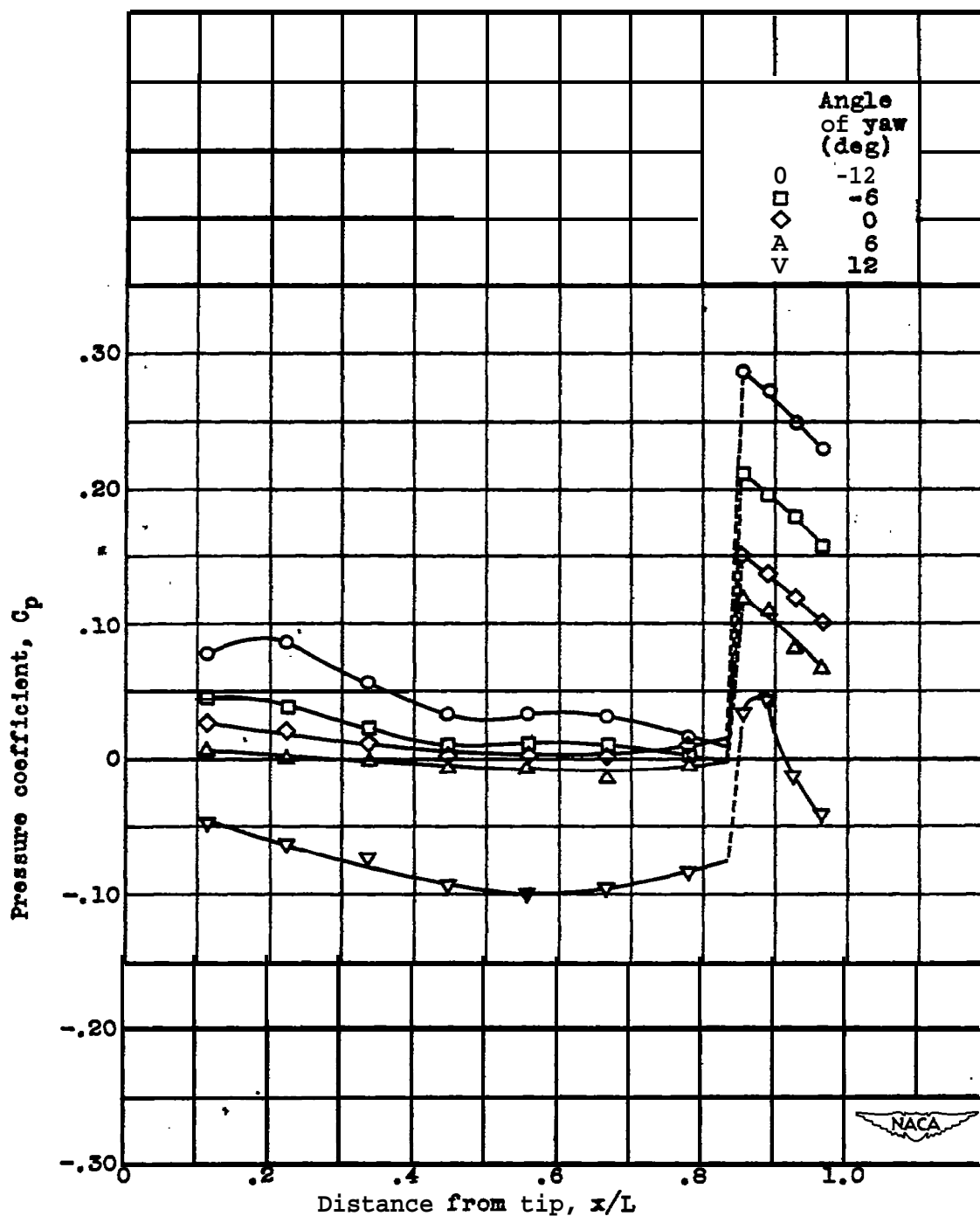
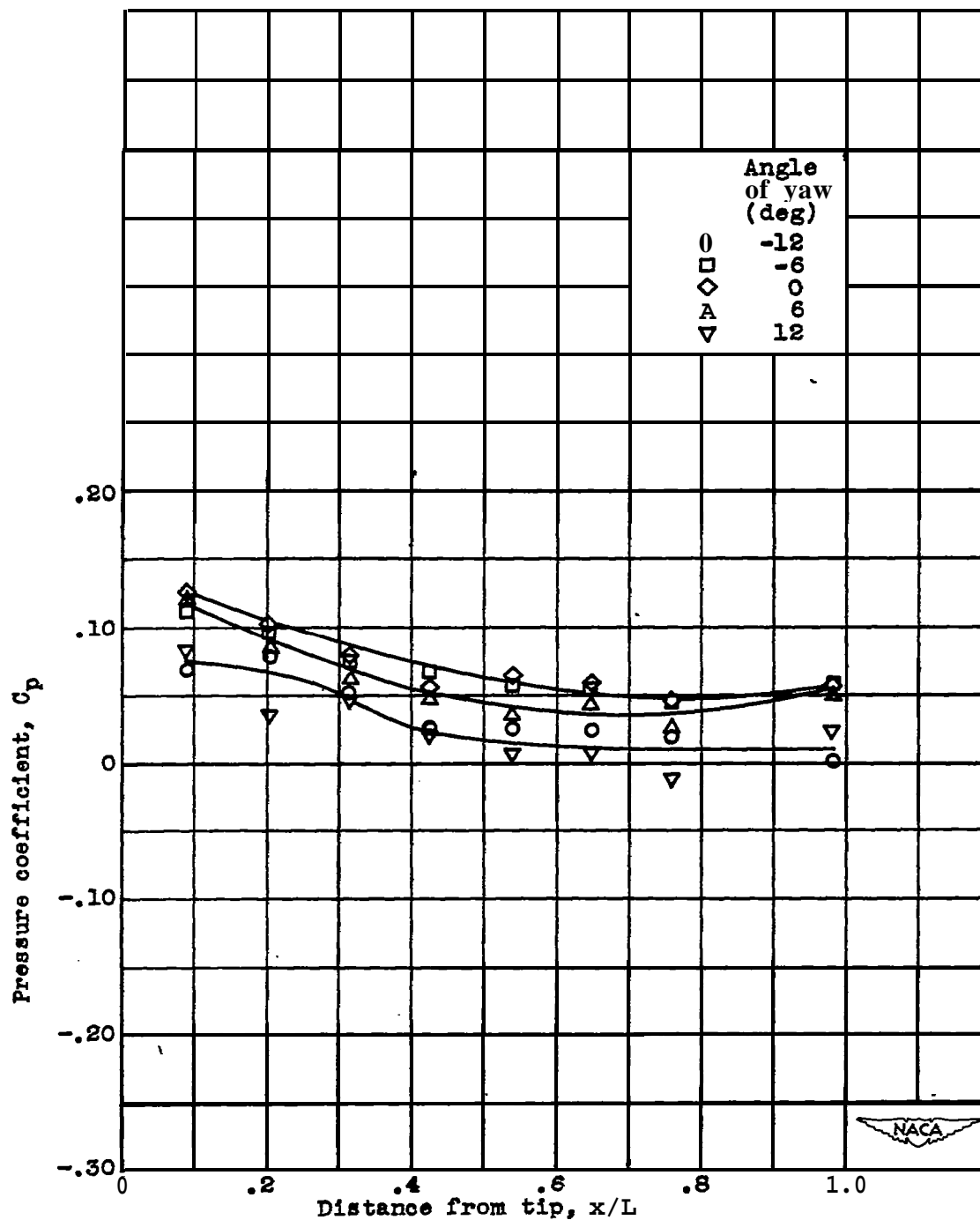
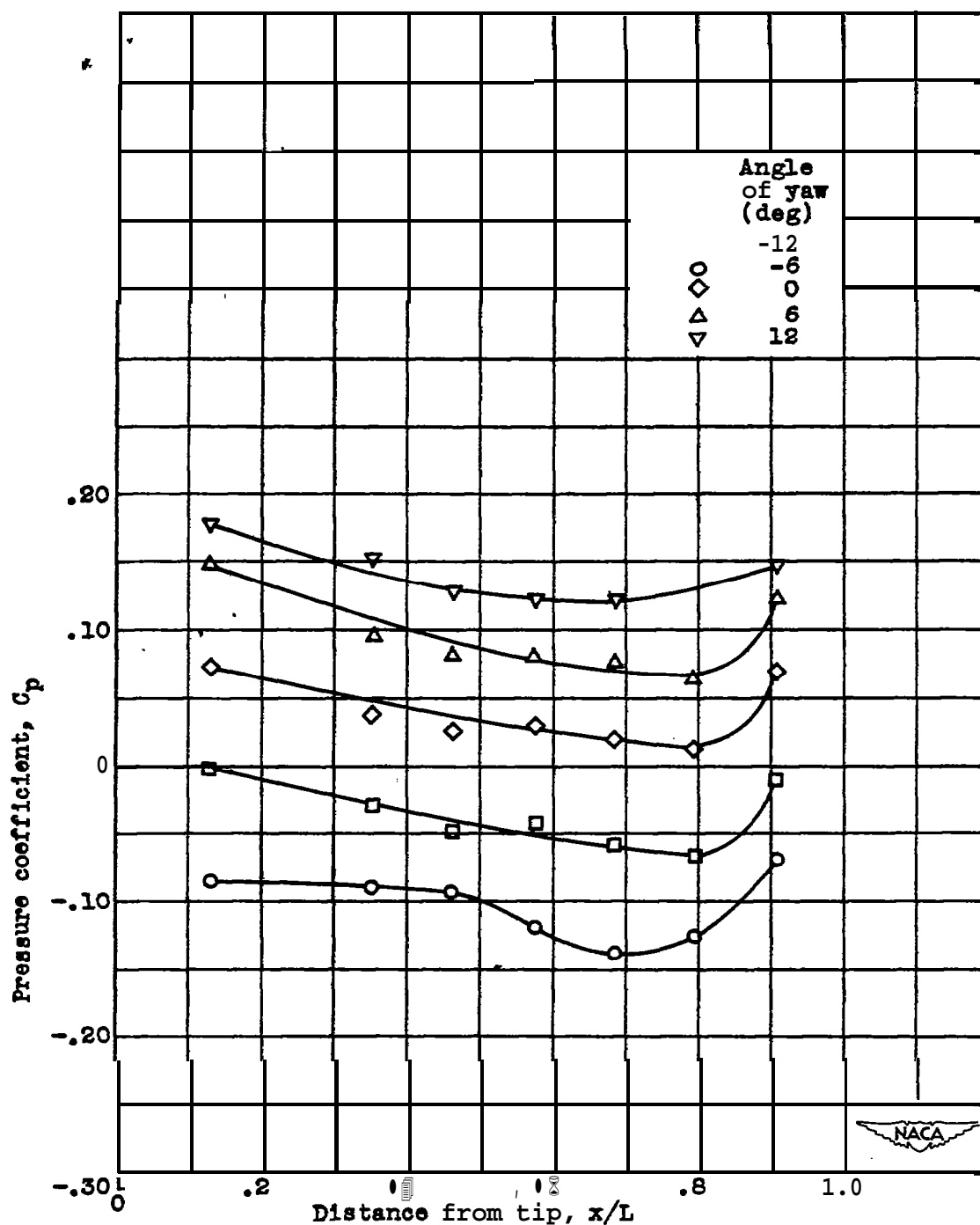


Figure 7. - Continued. Pressure distributions along longitudinal planes at 5 angle of attack for range of yaw angles.



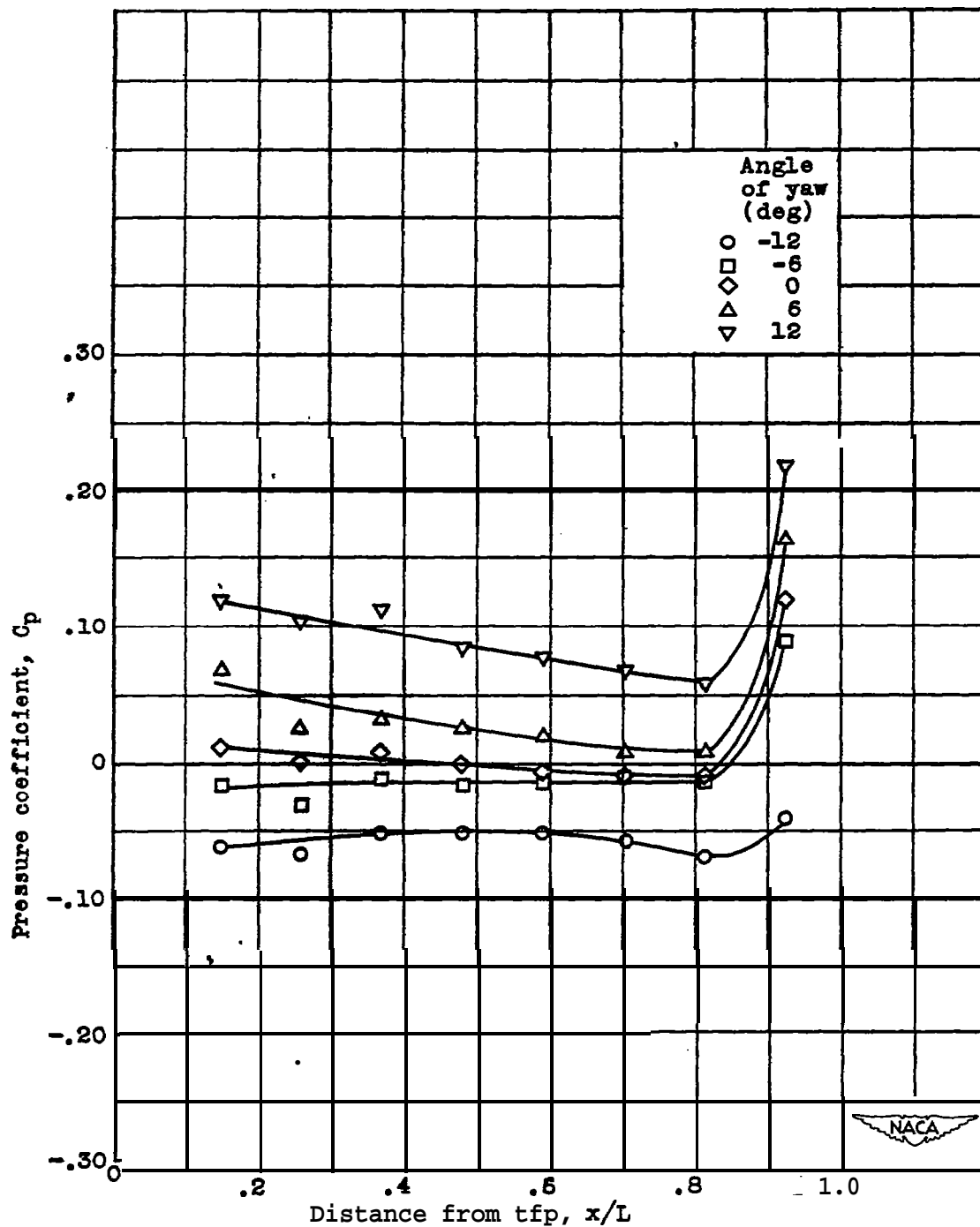
(c) $\theta = 180^\circ$ longitudinal plane.

Figure 7. - Continued. Pressure distributions along longitudinal planes at 5° angle of attack for range of yaw angles.



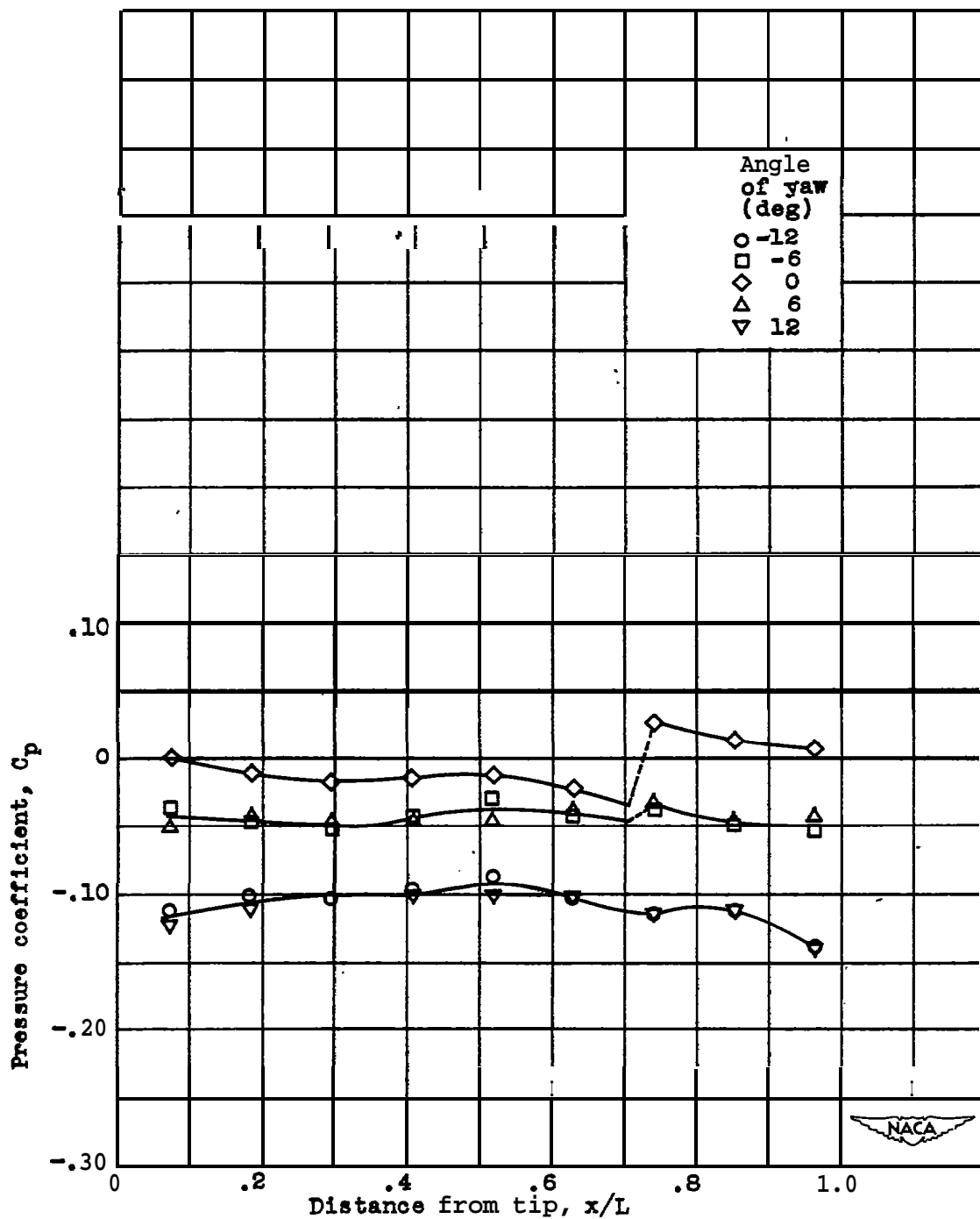
(d) $\theta = 225^\circ$ longitudinal plane.

Figure 7. - Continued. Pressure distributions along longitudinal planes at 5° angle of attack for range of yaw angles.



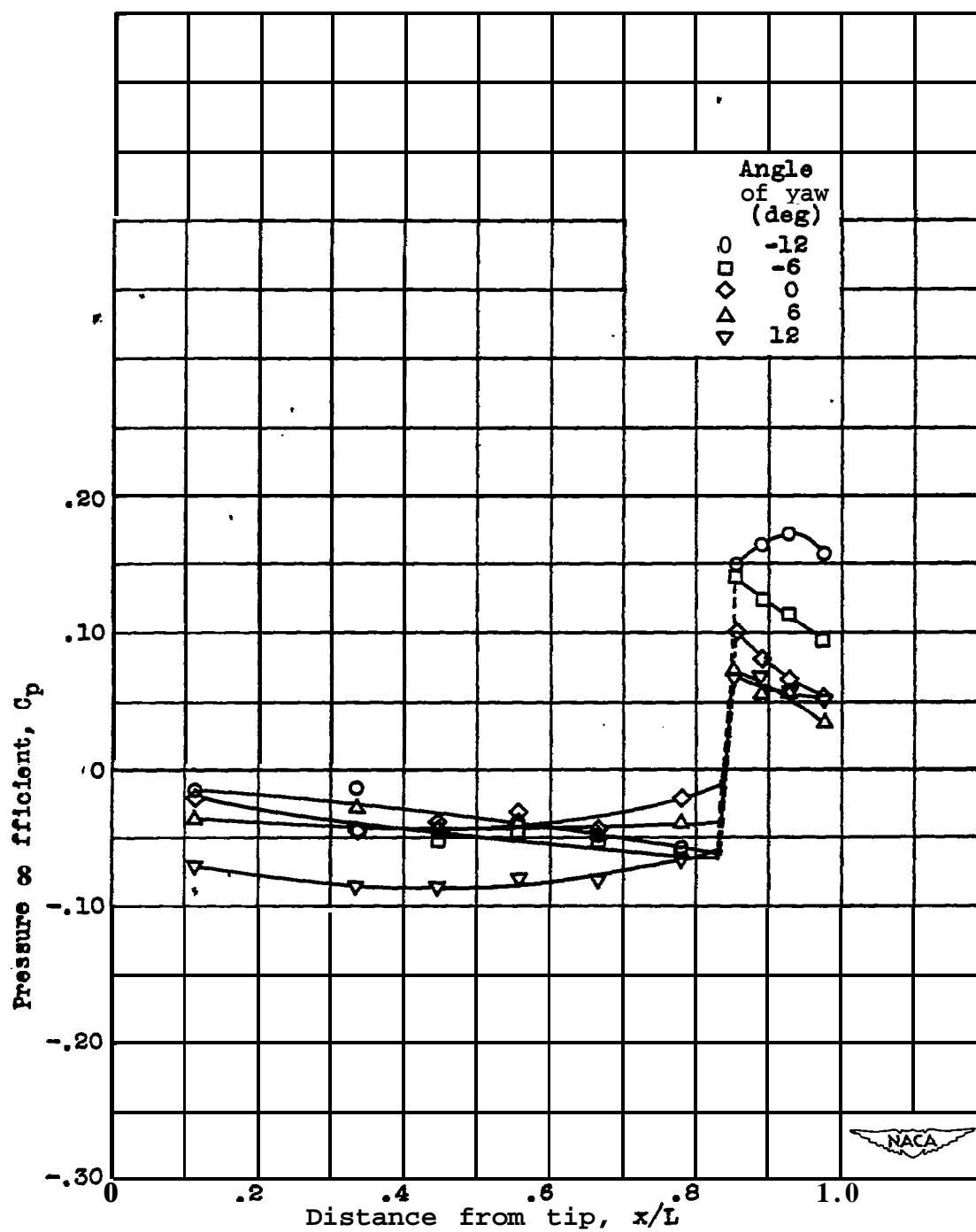
(e) $\theta = 270^\circ$ longitudinal plane.

Figure 7. - Concluded. Pressure distributions along longitudinal planes at 5° angle of attack for range of yaw angles.



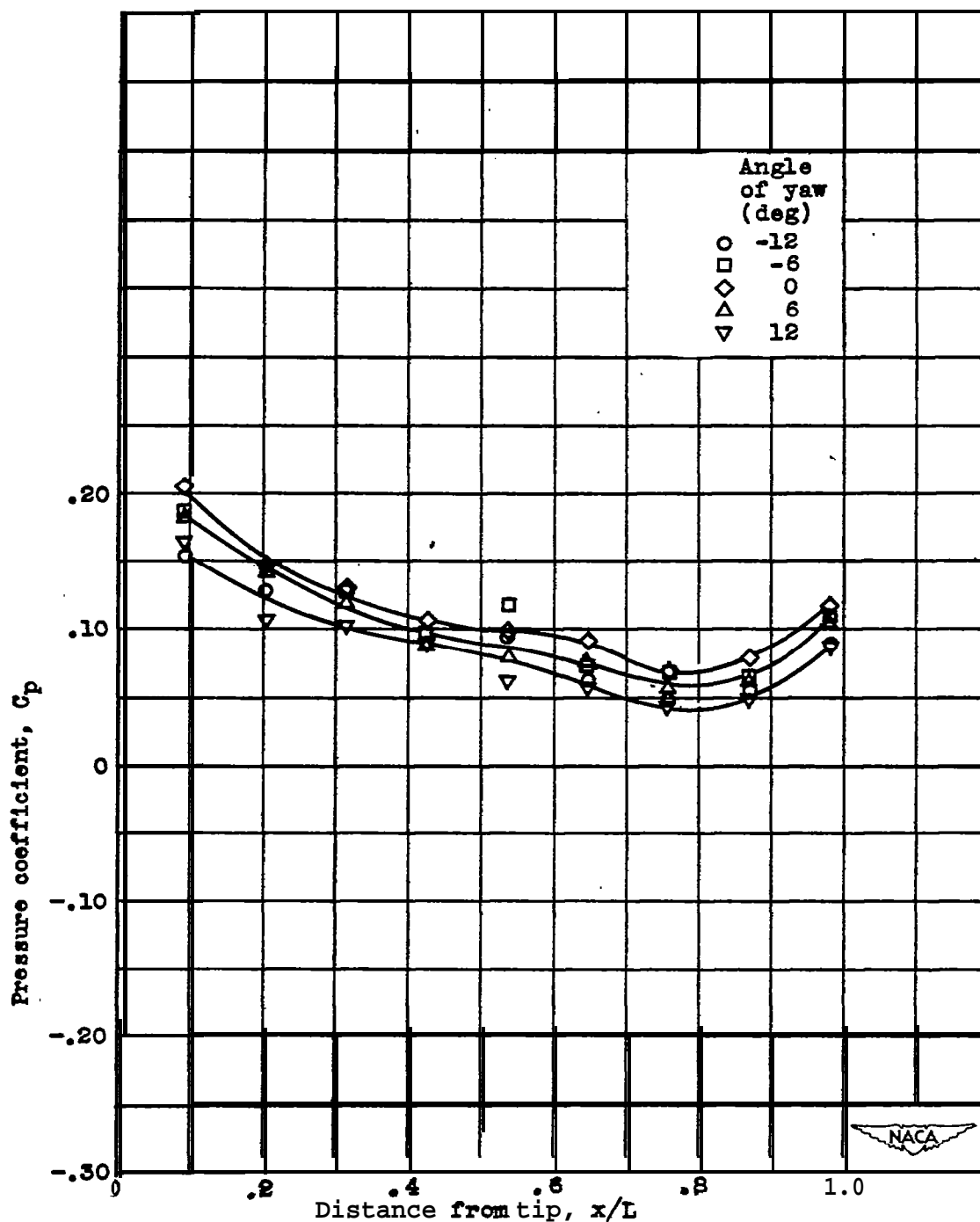
(a) $\theta = 0^\circ$ longitudinal plane.

Figure 8. - Pressure distributions along longitudinal planes at 10° angle of attack for range of yaw angles.



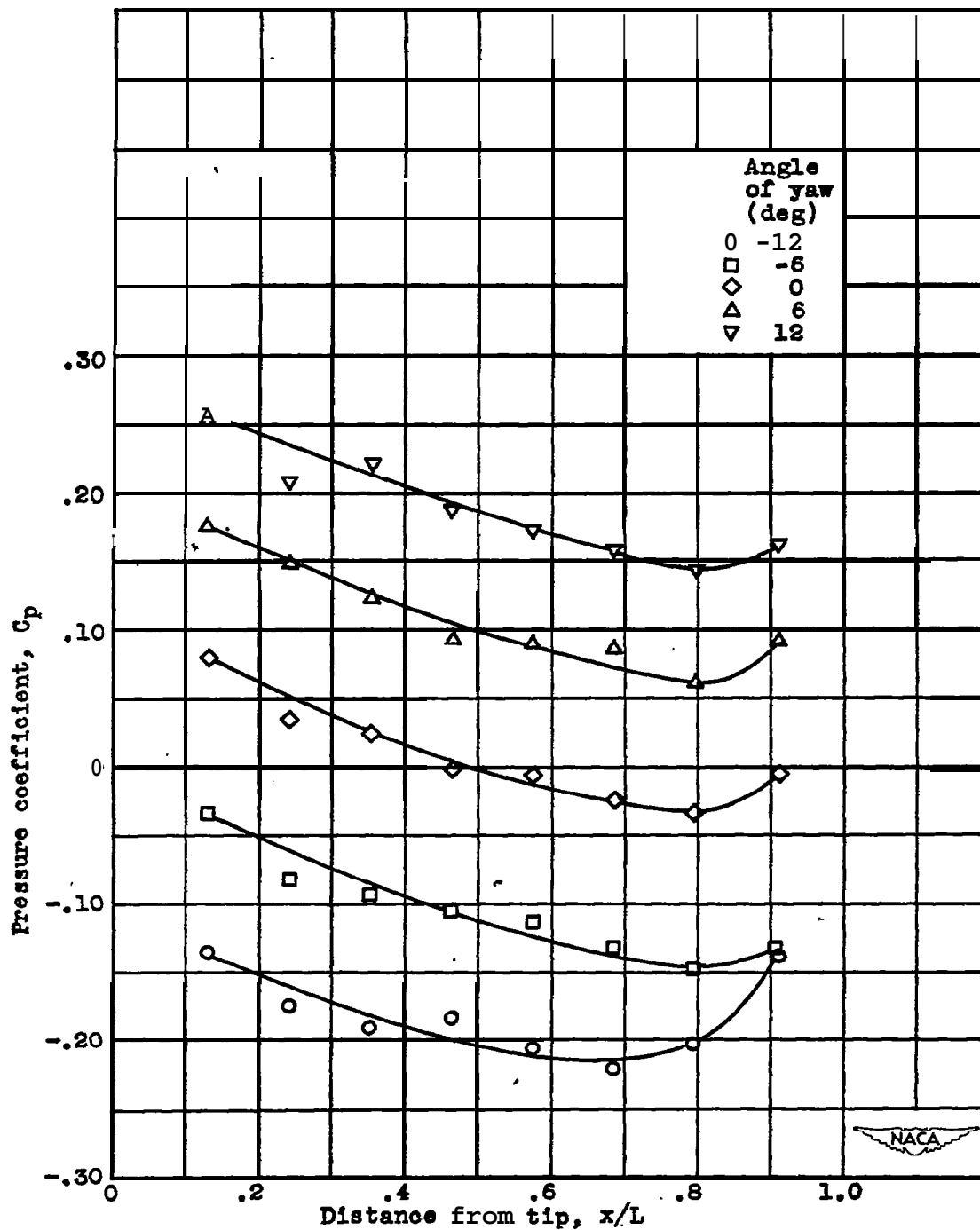
(b) $\theta = 45^\circ$ longitudinal plane.

Figure 8. - Continued. Pressure distributions along longitudinal planes at 10° angle of attack for range of yaw angles.



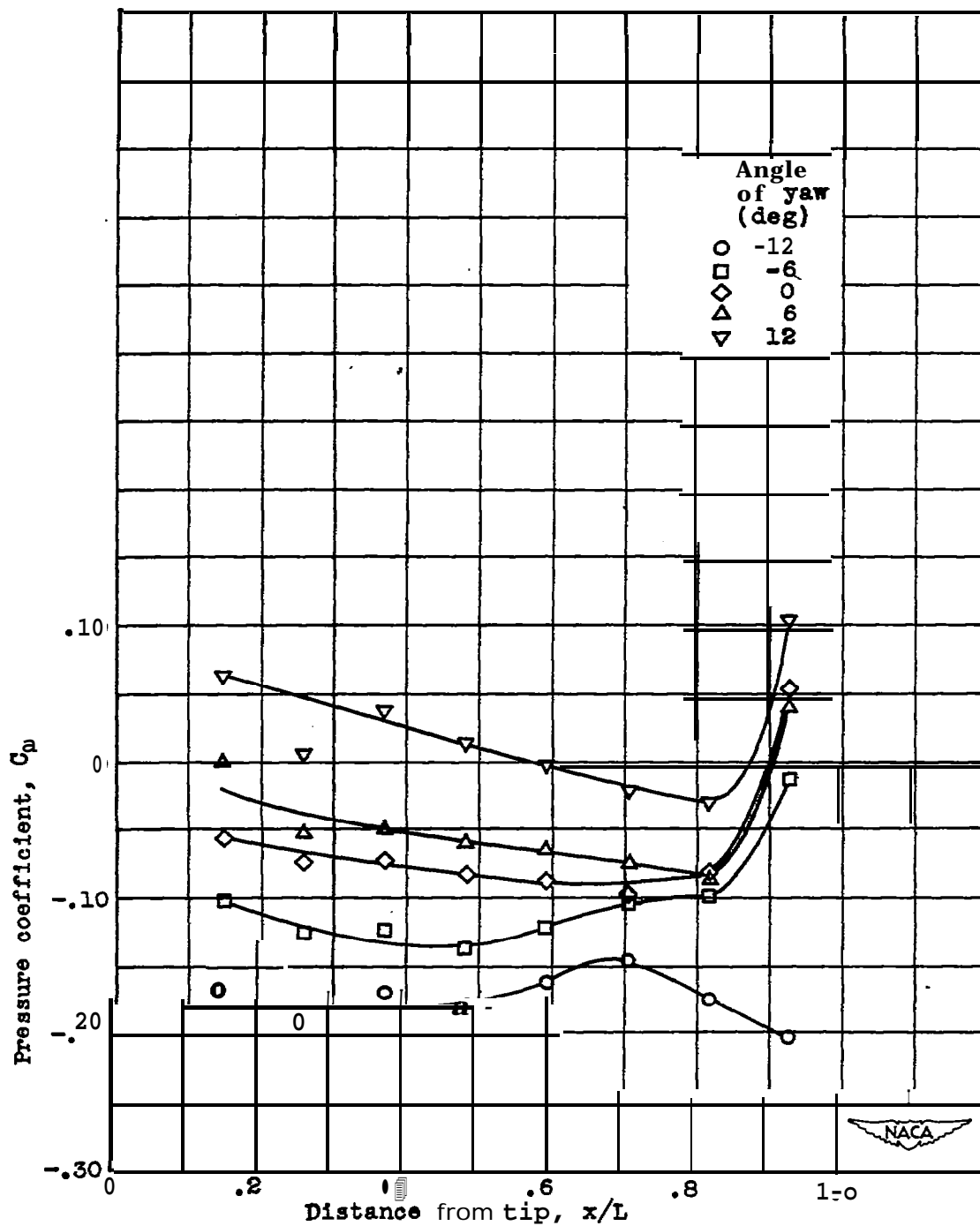
(a) $\theta = 180^\circ$ longitudinal plane.

Figure 8. - Continued. Pressure distributions along longitudinal planes at 10° angle of attack for range of yaw angles.



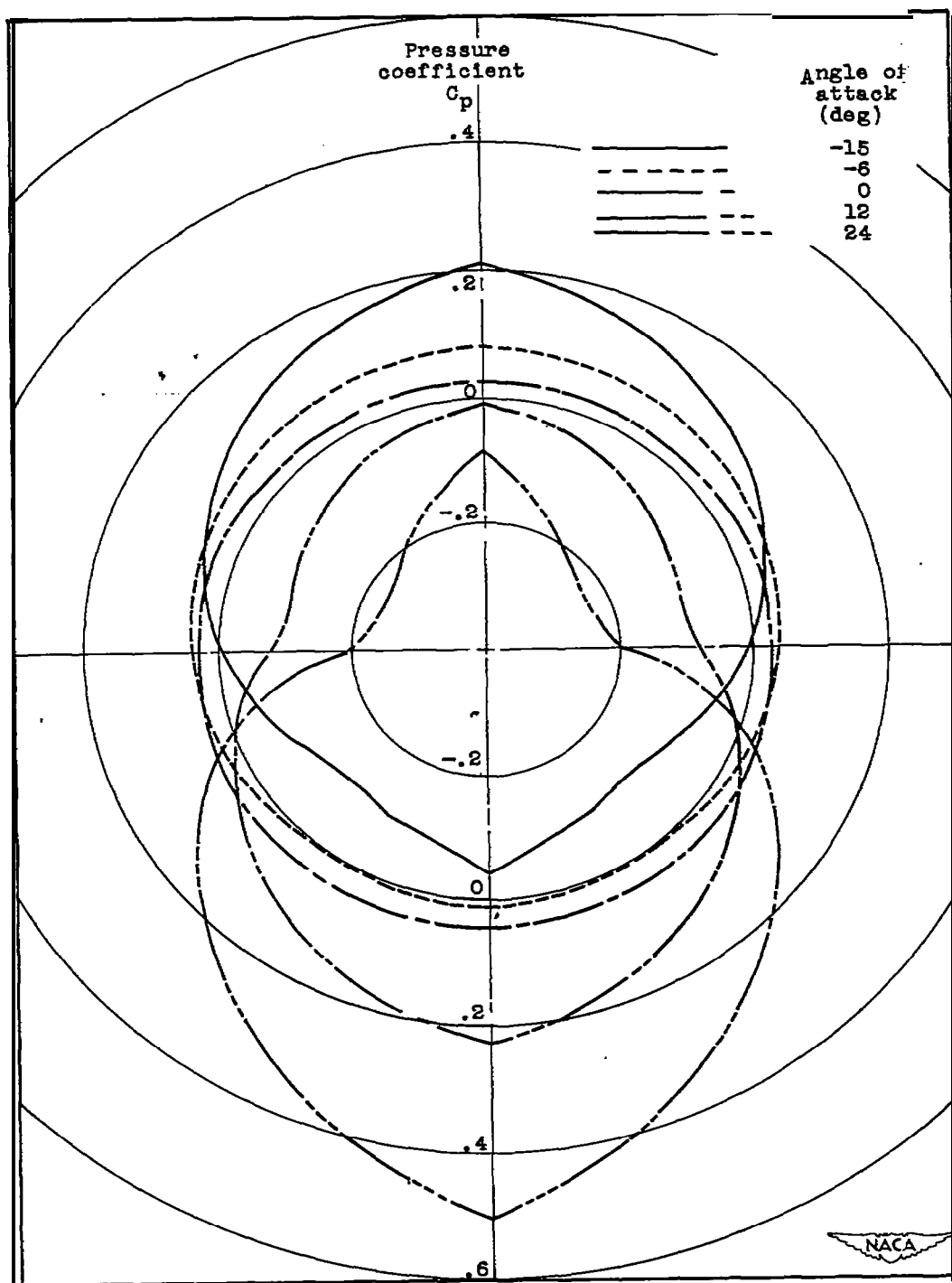
(d) $\theta = 225^\circ$ longitudinal plane.

Figure 8. - Continued. Pressure distributions along longitudinal planes at 10° angle of attack for range of yaw angles.



(e) $\theta = 270^\circ$ longitudinal plane.

Figure 8. - Concluded. Pressure distributions along longitudinal planes at 10° angle of attack for range of yaw angles,



(a) $x/L = 0.148$.

Figure 9. - Radial pressure distributions at 0° yaw angle for various angles of attack.

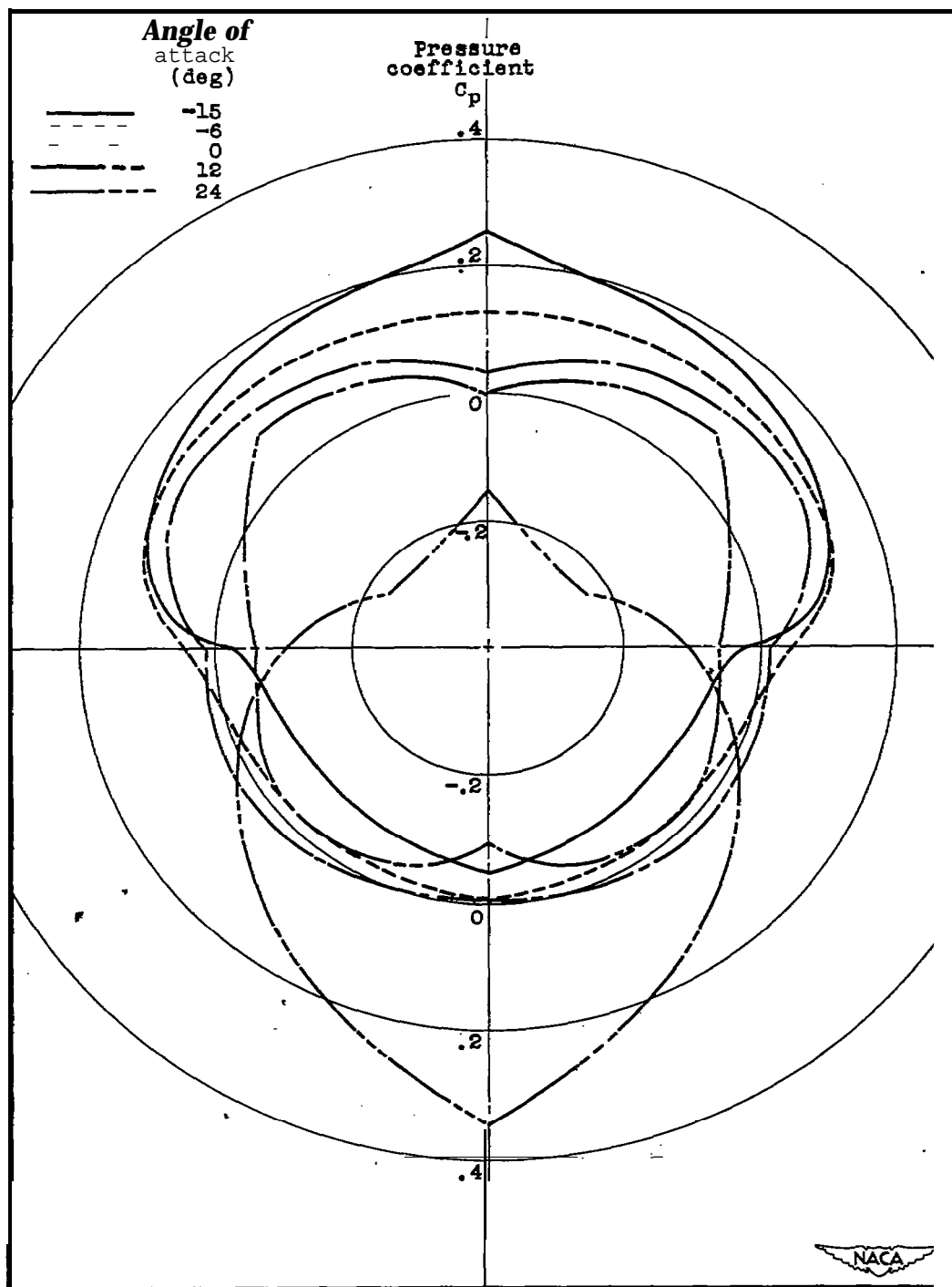
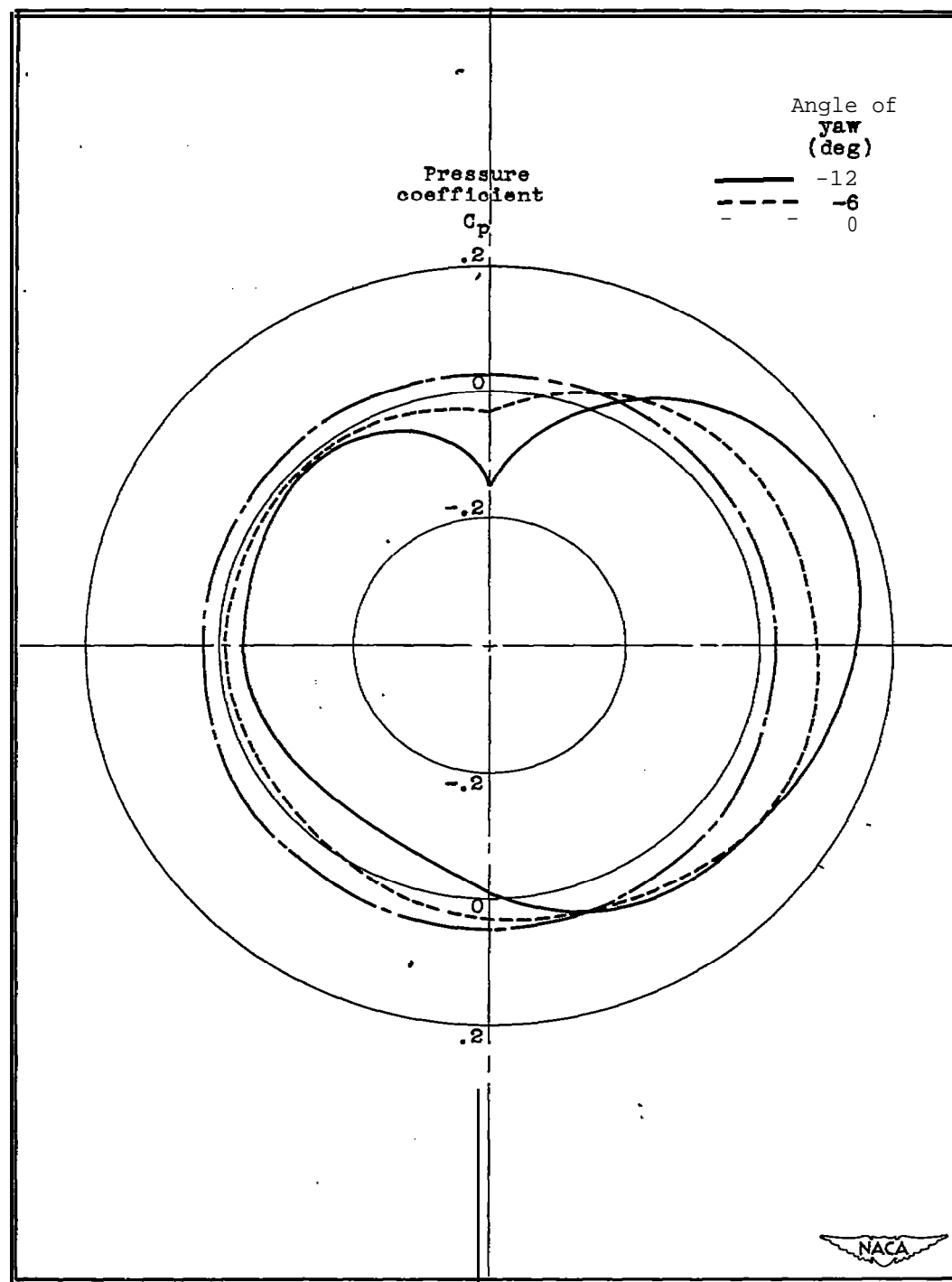
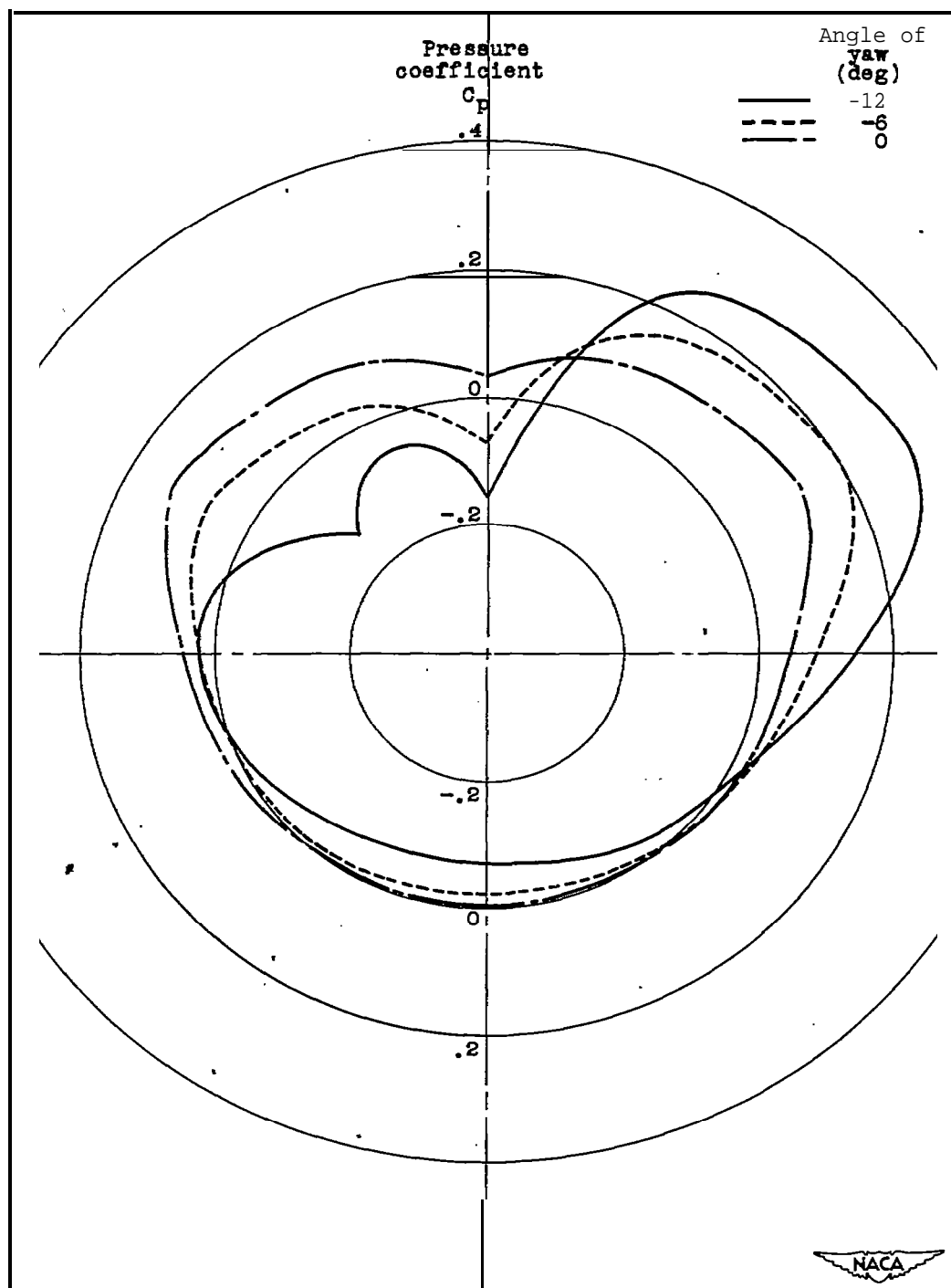


Figure 9. - Concluded. Radial pressure distributions at 0° yaw angle for various angles of attack.



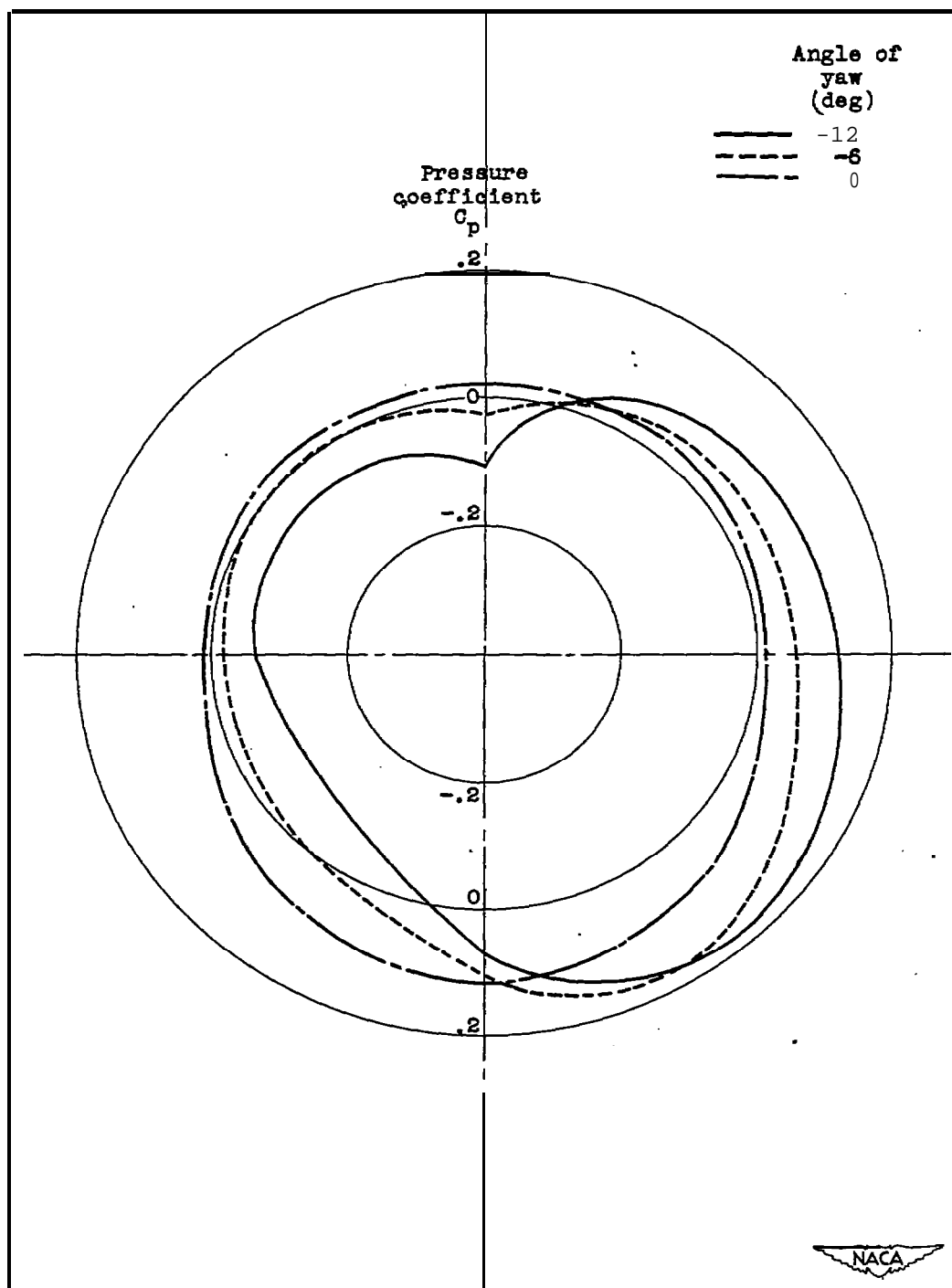
(a) $x/L = 0.148$.

Figure 10. - Radial pressure distributions at 0° angle of attack for three **yaw** angles,



(b) $x/L = 0.898$.

Figure 10. - Concluded. Radial pressure distributions at 0° angle of attack for three yaw angles.



(a) $x/L = 0.148$.

Figure 11. - Radial pressure distributions at 5° angle of attack for three yaw angles.

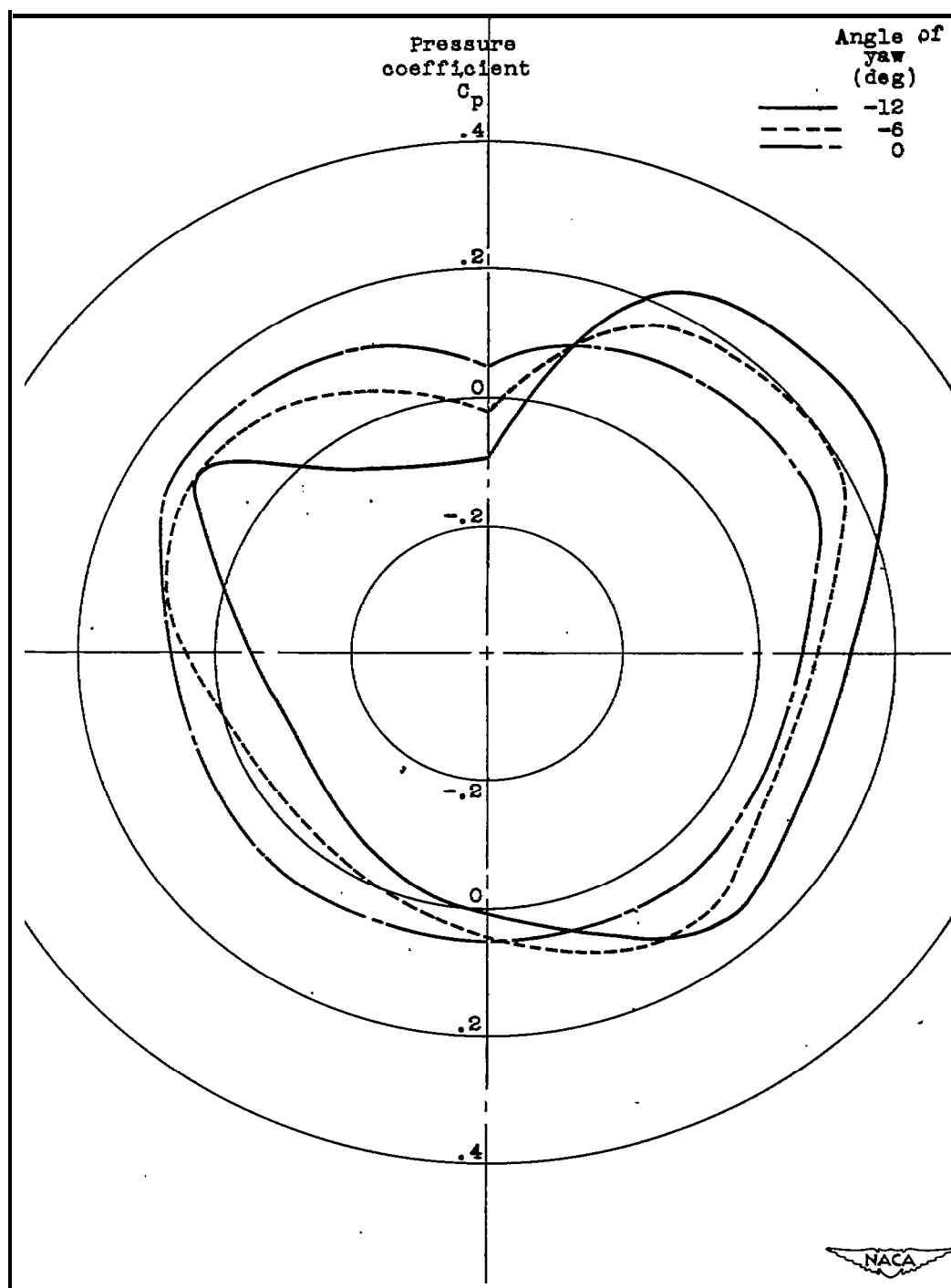
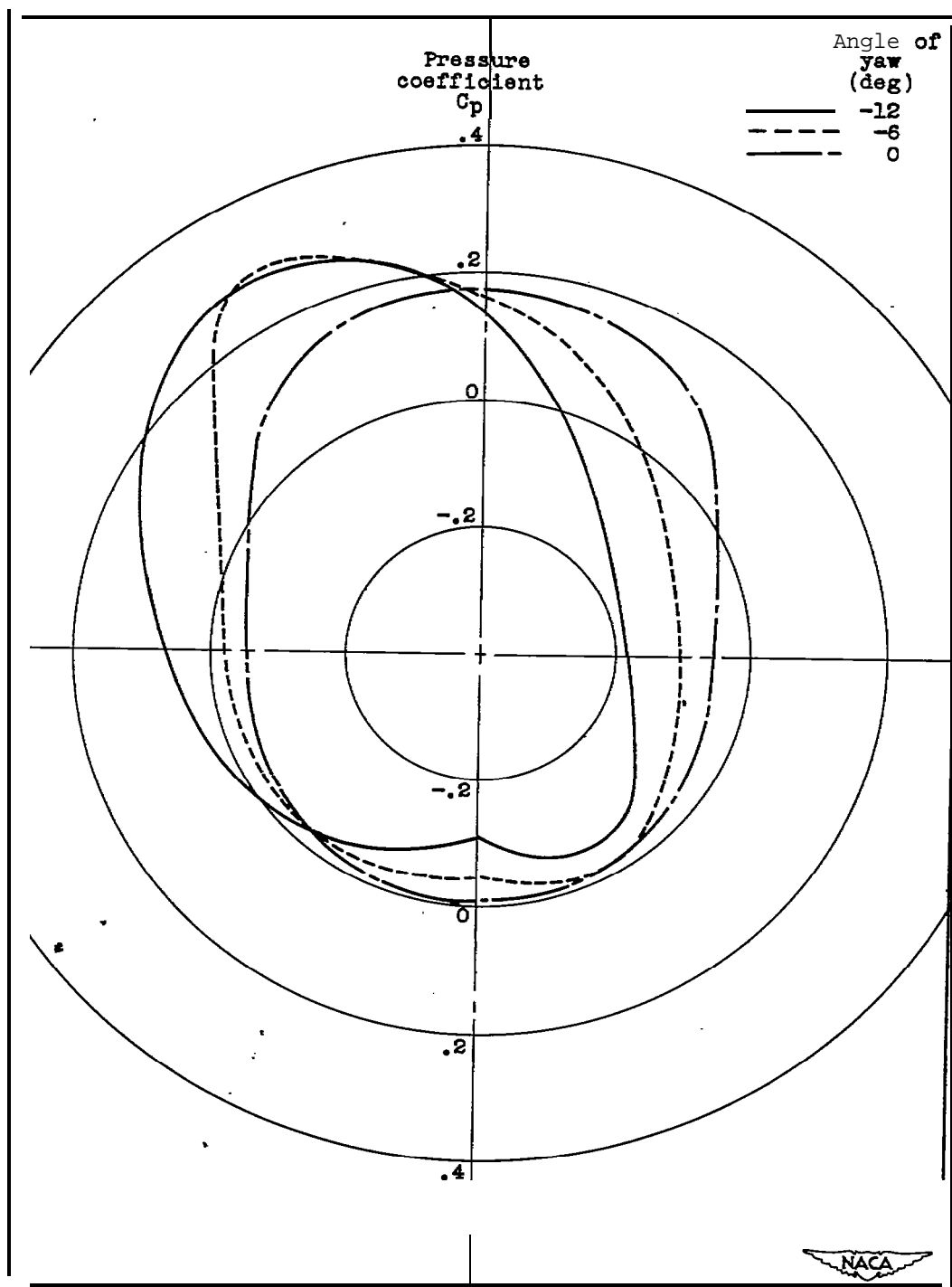
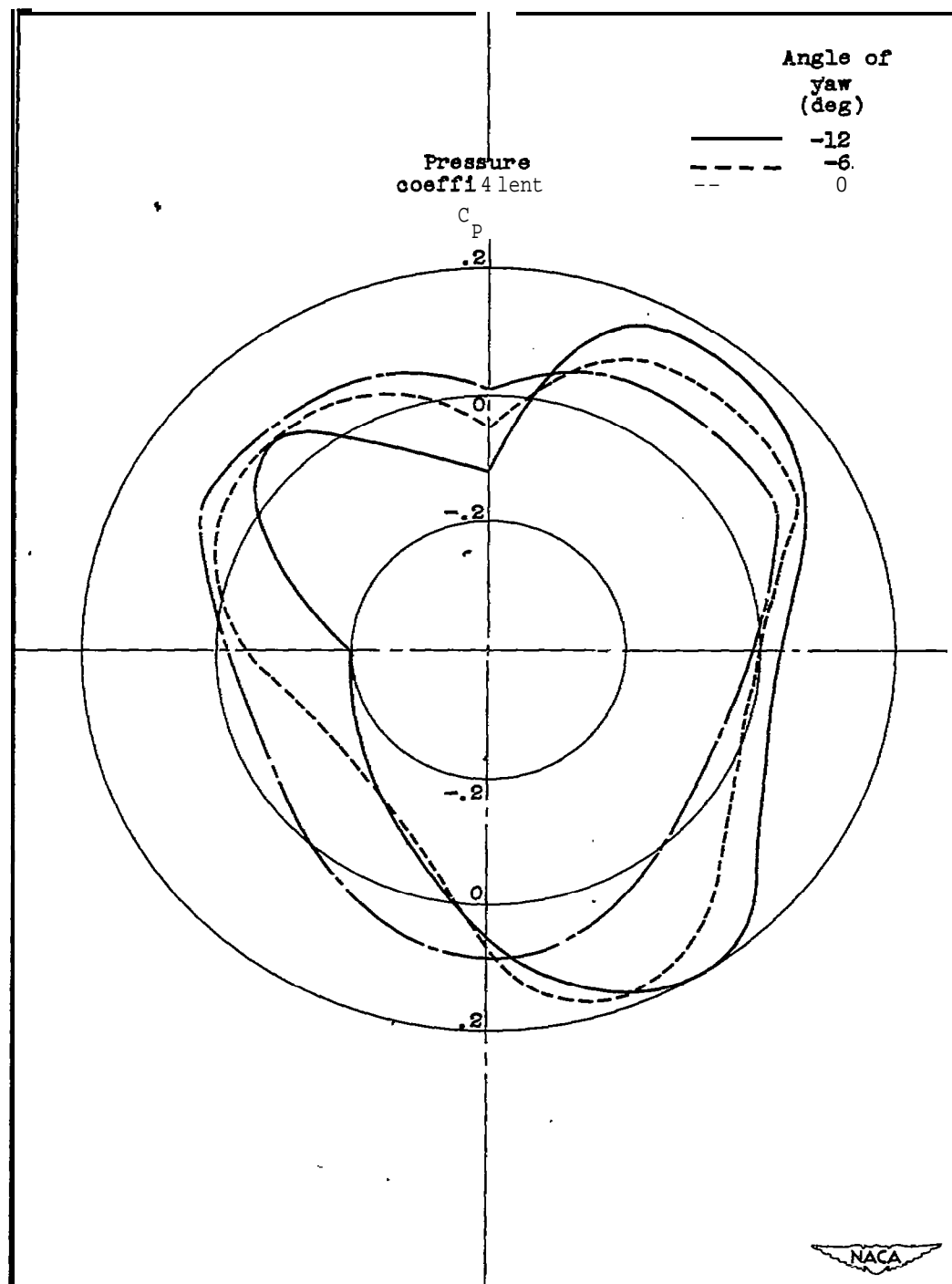


Figure 11, - Concluded. Radial pressure distributions at 5° angle of attack for three yaw angles.



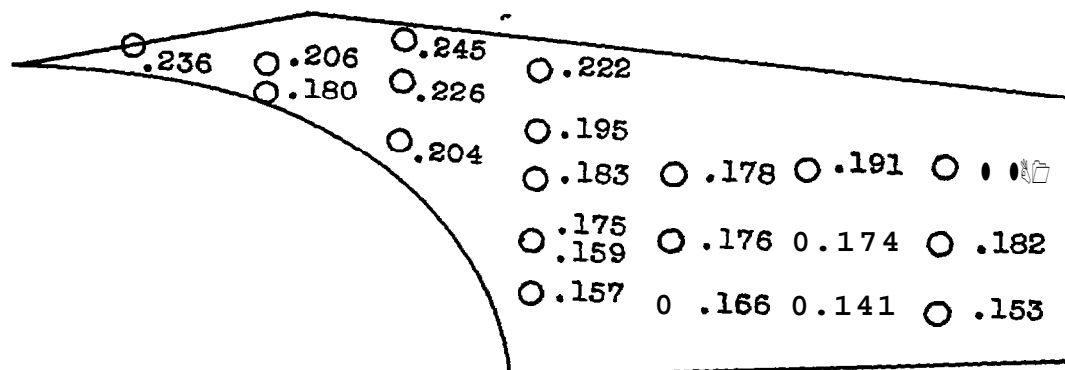
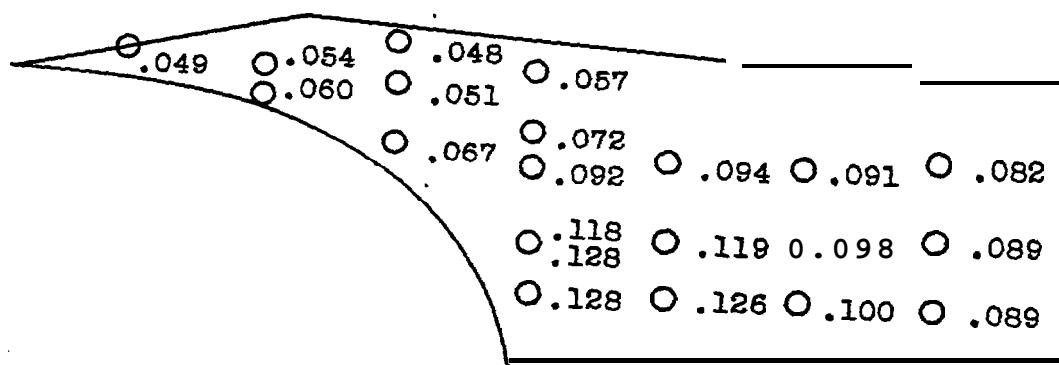
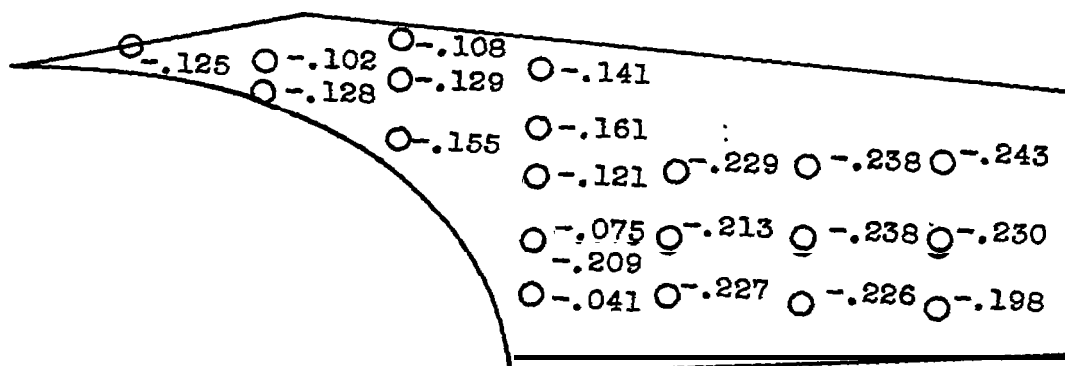
(a) $x/L = 0.148$.

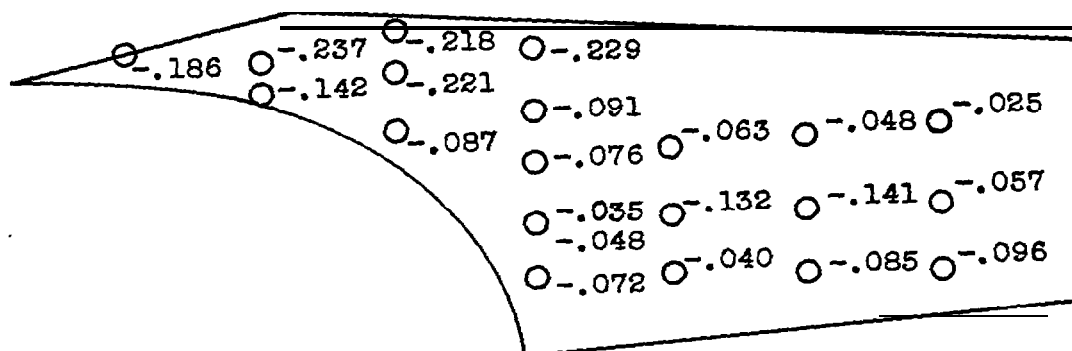
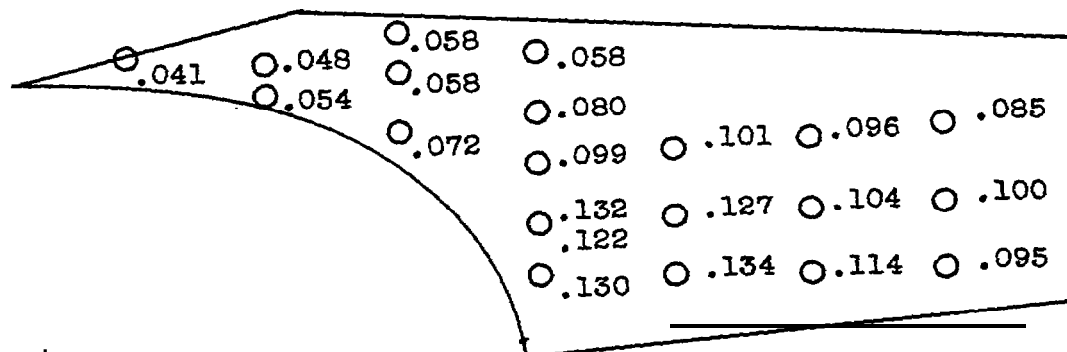
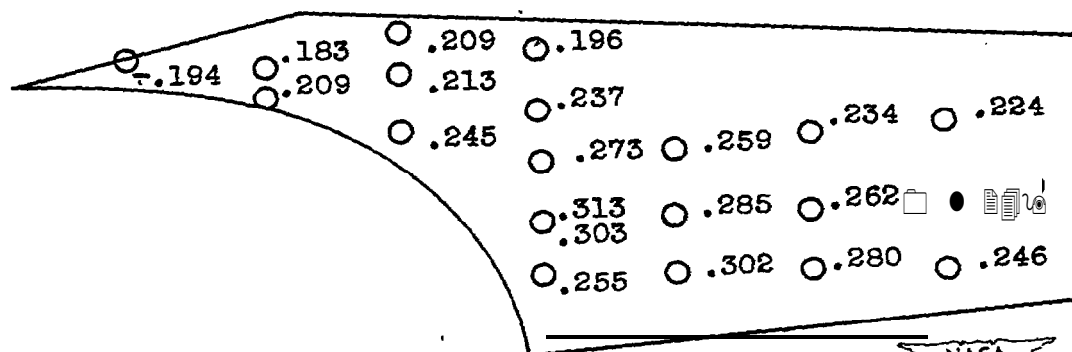
Figure 12. - Radial pressure distributions at 10° angle of attack for three yaw angles.

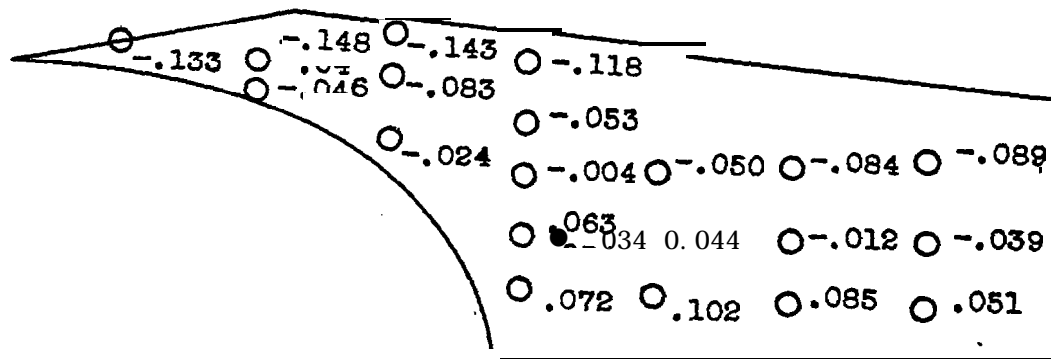


(b) $x/L = 0.898$.

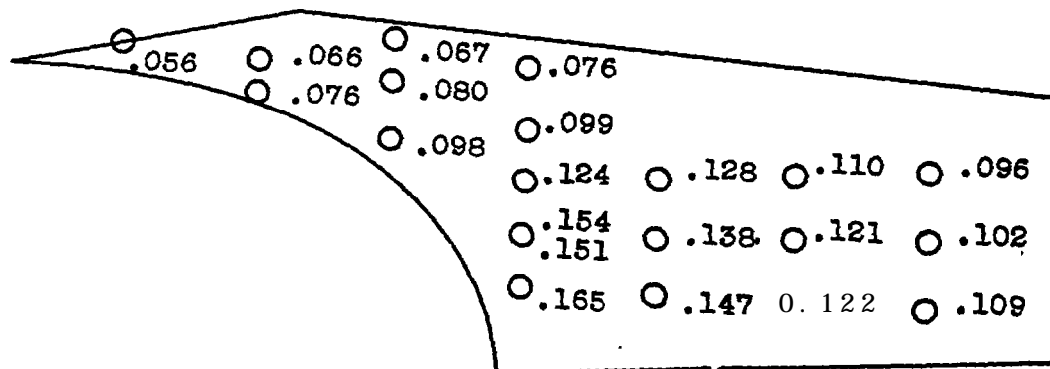
Figure 12. - Concluded. Radial pressure distributions at 10° angle of attack for three yaw angles.

(a) Angle of attack, -15° .(b) Angle of attack, 0° .(c) Angle of attack, 24° .Figure 13. Pressure coefficients on pilot canopy at 0° yaw angle for three angles of attack.

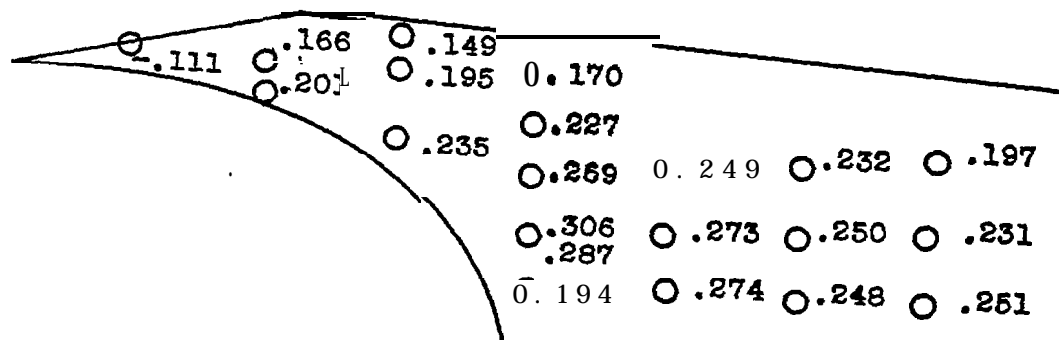
(a) Angle of yaw, -12° .(b) Angle of yaw, 0° .(c) Angle of yaw, 12° .Figure 14. - Pressure coefficients on pilot canopy at 0° angle of attack for three yaw angles.



(a) Angle of yaw, -12° .



(b) Angle of yaw, 0° .



(b) Angle of yaw, 12° .

Figure 15. - Pressure coefficients on pilot canopy at 5° angle of attack for three yaw angles,

NASA Technical Library



3 1176 01435 5565